

# Predictive Simulation of Global Instabilities in Tokamaks

Stephen C. Jardin  
Princeton Plasma Physics Laboratory

Fourth ITER International Summer School  
IISS 2010

Institute of Fusion Studies  
University of Texas at Austin

June 3, 2010

# Outline

Part 1: 2D tokamak instabilities and our ability to predict them with MHD equations

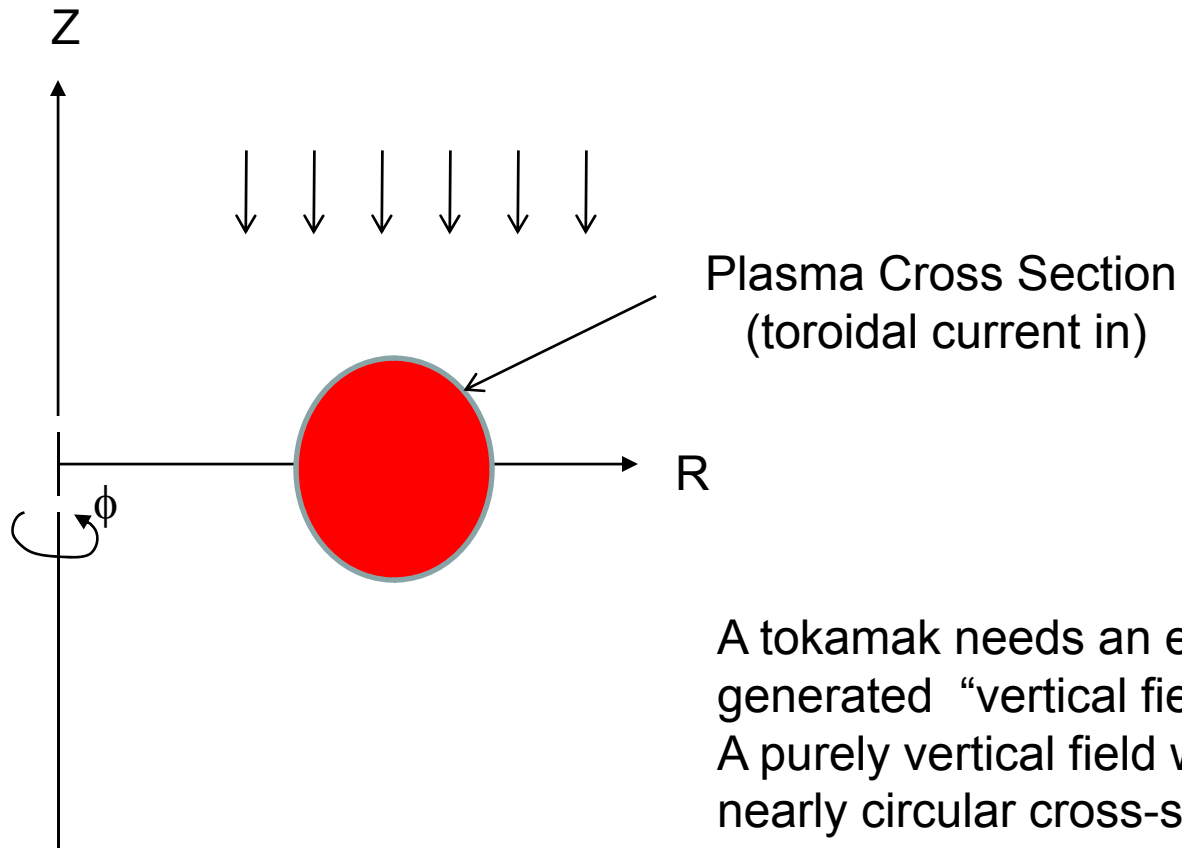
Part 2: 3D tokamak instabilities and our ability to predict them with MHD equations

# Outline

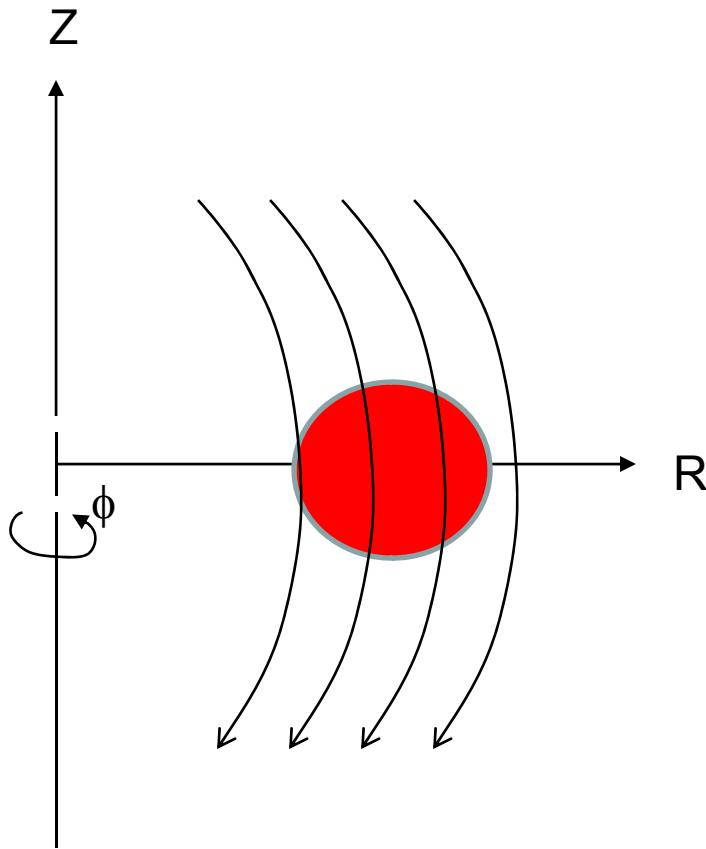
**Part I:** 2D tokamak instabilities and our ability to predict them with MHD equations

Part 2: 3D tokamak instabilities and our ability to predict them with MHD equations

## Tokamak Equilibrium Basics: Need for a vertical field

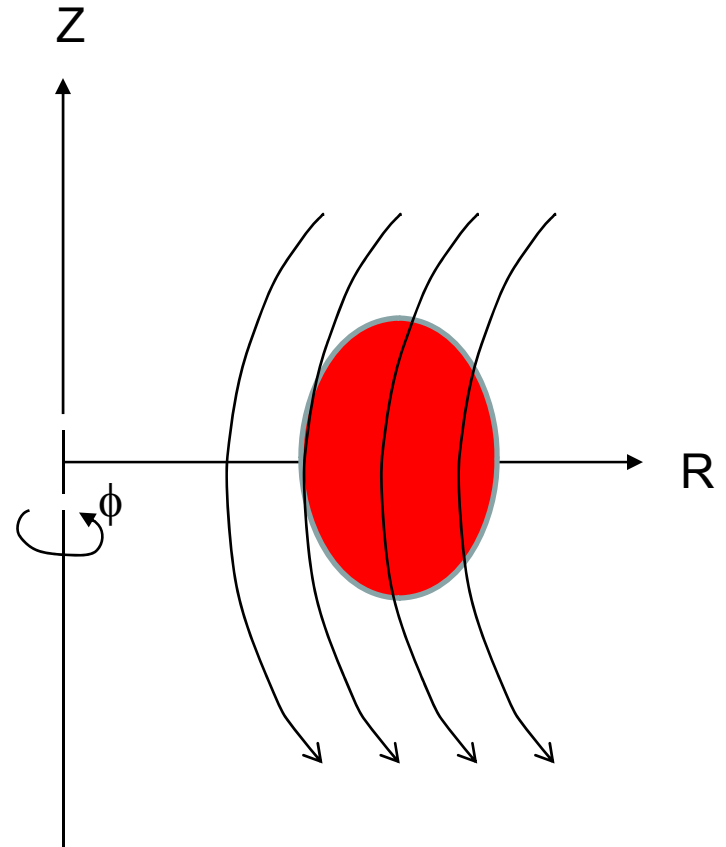


In actual tokamak experiments, external field is not purely straight but has some curvature to it



Good Curvature

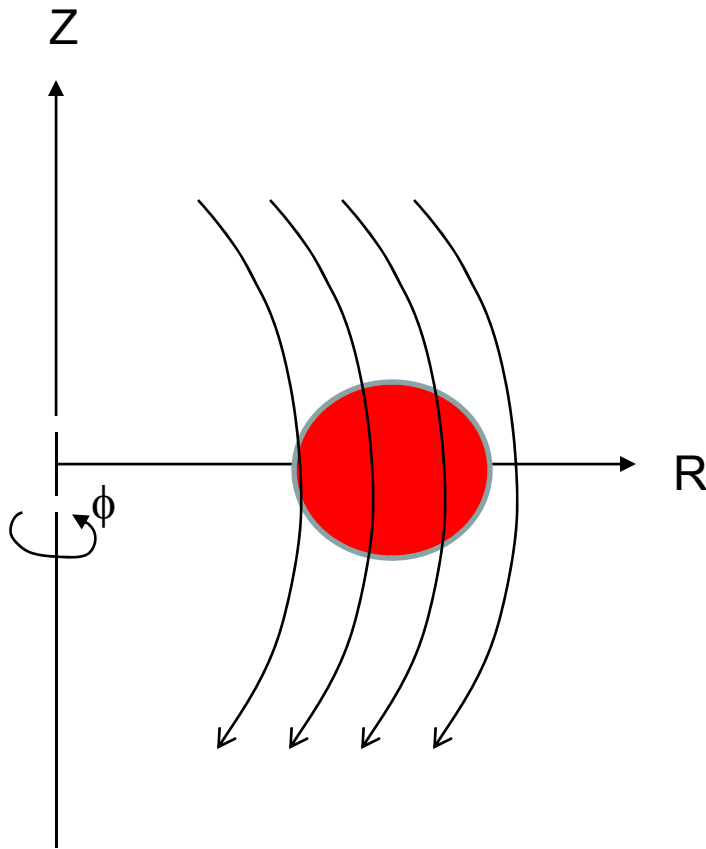
- Stable to vertical mode
- Oblate plasma
- low beta limits



Bad Curvature

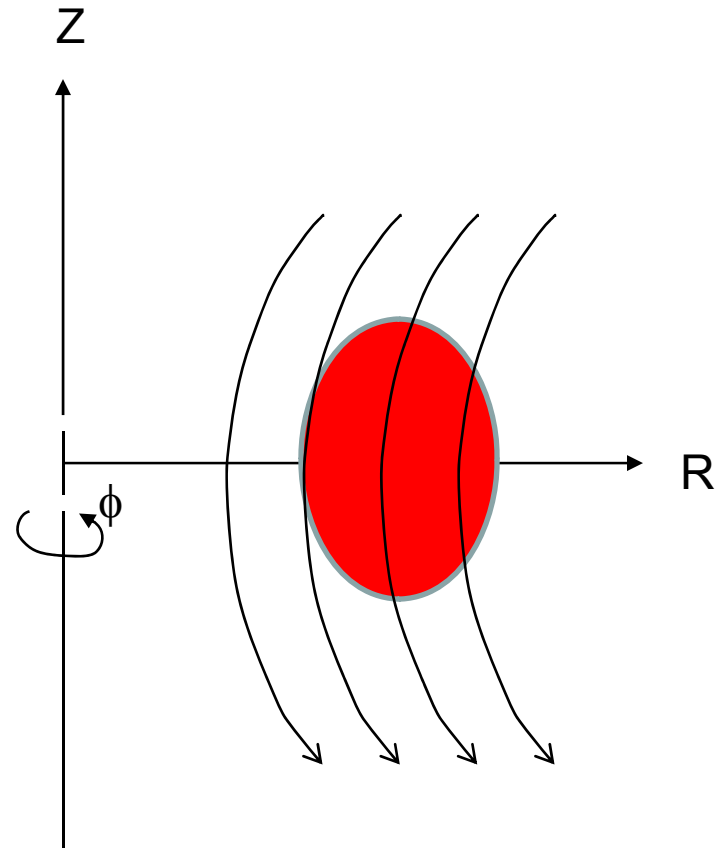
- Unstable to vertical mode
- Elongated plasma
- higher beta limits

In actual tokamak experiments, external field is not purely straight but has some curvature to it



Good Curvature

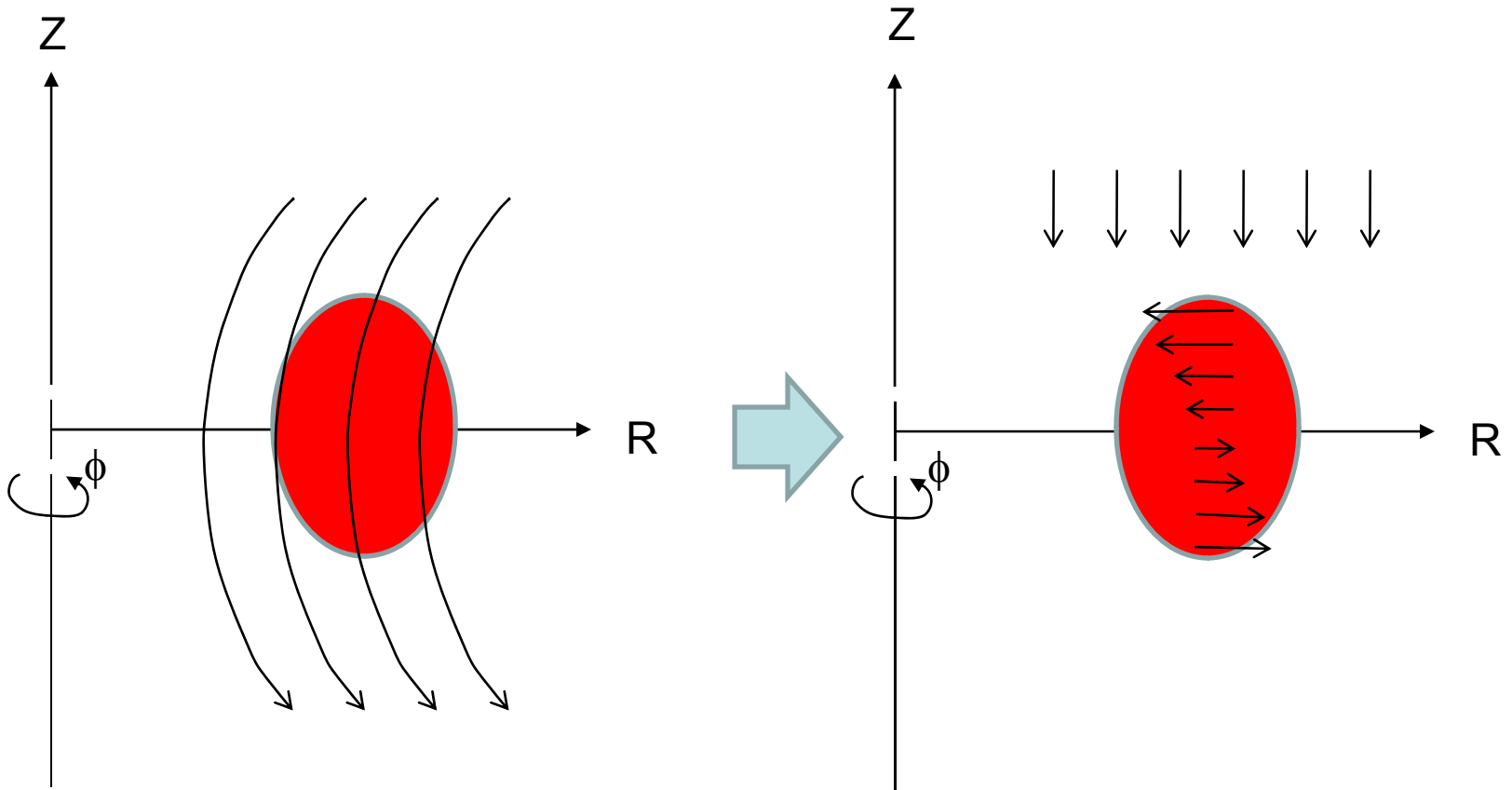
- Stable to vertical mode
- Oblate plasma
- low beta limits



Bad Curvature

- **Unstable to vertical mode**
- Elongated plasma
- higher beta limits

Field with curvature can be thought of as a superposition of vertical and radial field.



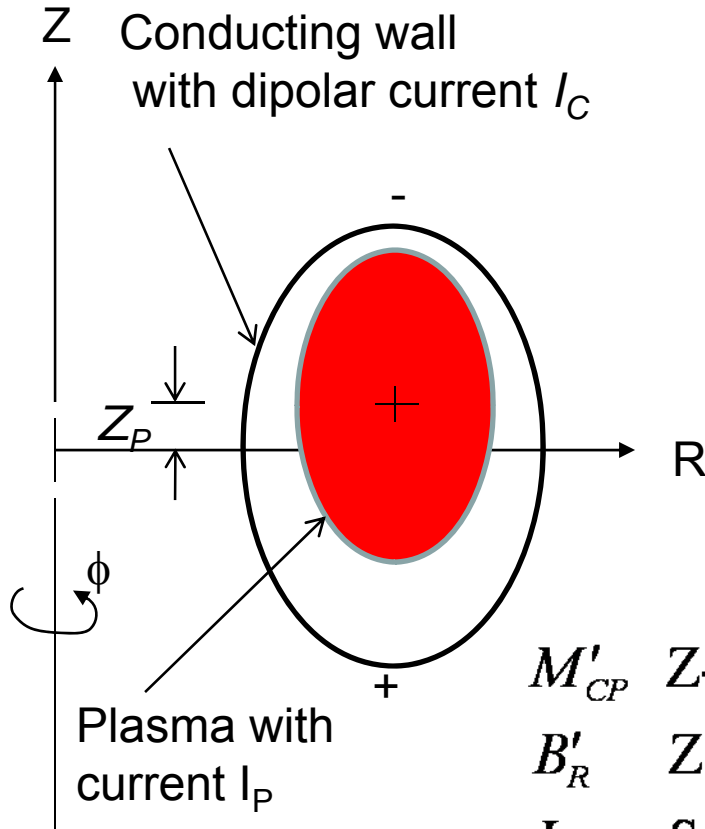
If plasma column is displaced upward, the force  
$$\mathbf{J} \times \mathbf{B} = I_P \times \mathbf{B}_{\text{Rext}}$$
will accelerate it further upward. Same for downward.

Vertical  
Instability

Alfven wave time scale: very fast!

A nearby conductor will produce eddy currents which act to stabilize

Describe the plasma as a rigid body of mass  $m$  with  $Z$  position  $Z_P$ . Assume time dependence  $e^{i\omega t}$



Equation of motion:

$$-m\omega^2 Z_P = I_P M'_{CP} I_C + I_P B'_R Z_P$$

inertia
conductor
external field

Circuit equation for wall:

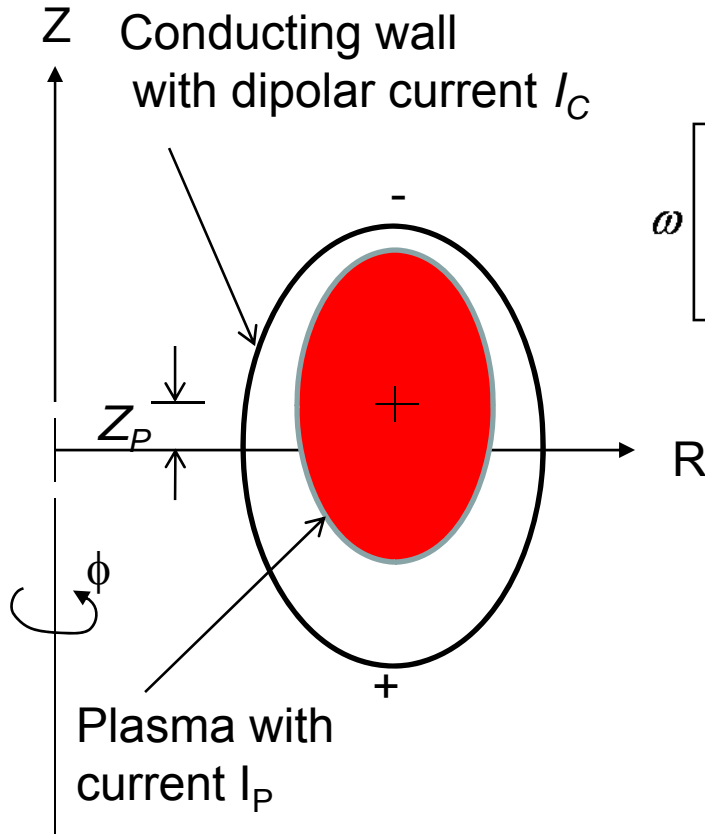
$$i\omega L I_C + R I_C + i\omega M'_{CP} I_P Z_P = 0$$

inductance
resistance
plasma coupling

- $M'_{CP}$  Z-derivative of plasma/wall mutual inductance
- $B'_R$  Z-derivative of external radial magnetic field
- $L$  Self-inductance of wall
- $R$  Resistance of wall



Introduce plasma velocity  $V_P = i \omega Z_P$  to get a 3x3 matrix eigenvalue equation for  $\omega$  of standard form



$$\omega \begin{bmatrix} i & 0 & 0 \\ 0 & im & 0 \\ iM'_{CP}I_P & 0 & iL \end{bmatrix} \begin{bmatrix} Z_P \\ V_P \\ I_C \end{bmatrix} = \begin{bmatrix} 0 & 1 & 0 \\ I_P B'_R & 0 & I_P M'_{CP} \\ 0 & 0 & -R \end{bmatrix} \begin{bmatrix} Z_P \\ V_P \\ I_C \end{bmatrix}$$

Three roots:

$$\omega_{1,2} = \pm \left[ \omega_S^2 - \omega_0^2 \right]^{1/2} + i \frac{\gamma_R}{2} \frac{\omega_S^2}{\left( \omega_S^2 - \omega_0^2 \right)}$$

$$\omega_3 = -i \frac{\gamma_R \omega_0^2}{\left( \omega_S^2 - \omega_0^2 \right)}$$

$$\gamma_R^2 \ll \omega_0^2, \omega_S^2$$

$$\gamma_R \equiv R / L$$

natural resistive decay rate of wall

$$\omega_0^2 \equiv I_P B'_R / m$$

destabilizing force

$$\omega_s^2 \equiv \left( I_P M'_{CP} \right)^2 / mL$$

stabilizing force from wall

With only passive conductor, still an unstable root but much smaller.  
 Not on Alfvén wave time scale but on L/R timescale of conductor.

$$\omega \begin{bmatrix} i & 0 & 0 \\ 0 & im & 0 \\ iM'_{CP}I_P & 0 & iL \end{bmatrix} \begin{bmatrix} Z_P \\ V_P \\ I_C \end{bmatrix} = \begin{bmatrix} 0 & 1 & 0 \\ I_P B'_R & 0 & I_P M'_{CP} \\ 0 & 0 & -R \end{bmatrix} \begin{bmatrix} Z_P \\ V_P \\ I_C \end{bmatrix}$$

These are high frequency ( $\sim 10^{-7}$  sec) stable oscillations that are slowly damped by the wall resistivity

This is the unstable mode. Very slow ( $\sim 10^{-1}$  sec), and independent of plasma mass.

Three roots:

$$\omega_{1,2} = \pm \left[ \omega_S^2 - \omega_0^2 \right]^{1/2} + i \frac{\gamma_R}{2} \frac{\omega_S^2}{\left( \omega_S^2 - \omega_0^2 \right)}$$

$$\omega_3 = -i \frac{\gamma_R \omega_0^2}{\left( \omega_S^2 - \omega_0^2 \right)}$$

$$\gamma_R^2 \ll \omega_0^2, \omega_S^2$$

$$\gamma_R \equiv R/L$$

natural resistive decay rate of wall

$$\omega_0^2 \equiv I_P B'_R / m$$

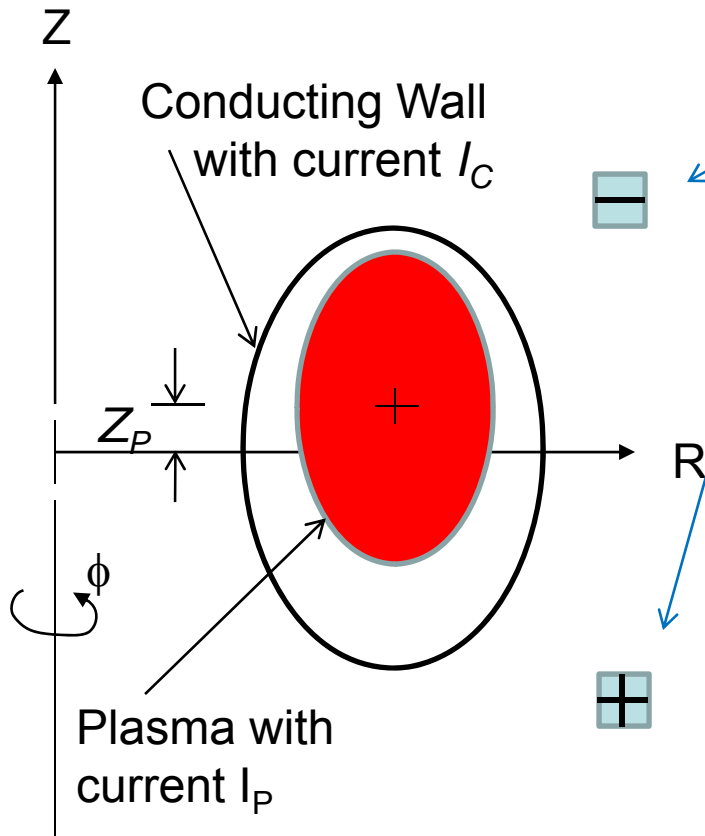
destabilizing force

$$\omega_S^2 > \omega_0^2$$

$$\omega_s^2 \equiv (I_P M'_{CP})^2 / mL$$

stabilizing force from wall

Total stability is obtained by adding an active feedback system which only needs to act on this slower timescale.



This “rigid” mode is easily stabilized by adding a pair of feedback coils of opposite sign, and applying a voltage proportional to the plasma displacement -or its time integral or time derivative (PID)

Three roots:

$$\omega_{1,2} = \pm \left[ \omega_S^2 - \omega_0^2 \right]^{1/2} + i \frac{\gamma_R}{2} \frac{\omega_S^2}{\left( \omega_S^2 - \omega_0^2 \right)}$$

$$\omega_3 = -i \frac{\gamma_R \omega_0^2}{\left( \omega_S^2 - \omega_0^2 \right)}$$

$$\gamma_R^2 \ll \omega_0^2, \omega_S^2$$

$$\gamma_R \equiv R / L$$

natural resistive decay rate of wall

$$\omega_0^2 \equiv I_P B'_R / m$$

destabilizing force

$$\omega_s^2 \equiv \left( I_P M'_{CP} \right)^2 / mL$$

stabilizing force from wall

To model this “vertical instability” in realistic geometry, and take the non-rigid motion of the plasma into account, we take advantage of the fact that the unstable mode does not depend on the plasma mass (or inertia), and the stable modes are very high frequency and low amplitude.

$$\frac{\partial \mathbf{B}}{\partial t} = -\nabla \times \mathbf{E}$$

$$nM_i \left( \frac{\partial \mathbf{V}}{\partial t} + \mathbf{V} \cdot \nabla \mathbf{V} \right) + \nabla p = \mathbf{J} \times \mathbf{B}$$

$$\mathbf{E} + \mathbf{V} \times \mathbf{B} = \eta \mathbf{J}$$

$$\frac{3}{2} \frac{\partial p}{\partial t} + \nabla \cdot \left( \frac{3}{2} p \mathbf{V} \right) = -p \nabla \cdot \mathbf{V} + \eta J^2$$

$$\mathbf{J} = \nabla \times \mathbf{B}$$

We start with the basic MHD + circuit equations and apply a “resistive timescale ordering”

Introduce small parameter  $\varepsilon \ll 1$

$$\frac{\partial}{\partial t} \sim \mathbf{V} \sim \mathbf{E} \sim V_i \sim \eta \sim R \sim \varepsilon$$

$$\frac{d}{dt} \left[ L_i I_i + \sum_{i \neq j} M_{ij} I_j + \int_P J_\phi G(R_i, R) dR \right] + R_i I_i = V_i$$

To model this “vertical instability” in realistic geometry, and taking the non-rigid motion of the plasma into account, we take advantage of the fact that the unstable mode does not depend on the plasma mass (or inertia), and the stable modes are very high frequency and low amplitude.

$$\frac{\partial \mathbf{B}}{\partial t} = -\nabla \times \mathbf{E}$$

$$\varepsilon^2 n M_i \left( \frac{\partial \mathbf{V}}{\partial t} + \mathbf{V} \cdot \nabla \mathbf{V} \right) + \nabla p = \mathbf{J} \times \mathbf{B}$$

$$\mathbf{E} + \mathbf{V} \times \mathbf{B} = \eta \mathbf{J}$$

$$\frac{3}{2} \frac{\partial p}{\partial t} + \nabla \cdot \left( \frac{3}{2} p \mathbf{V} \right) = -p \nabla \cdot \mathbf{V} + \eta J^2$$

$$\mathbf{J} = \nabla \times \mathbf{B}$$

$$\frac{d}{dt} \left[ L_i I_i + \sum_{i \neq j} M_{ij} I_j + \int_P J_\phi G(R_i, R) dR \right] + R_i I_i = V_i$$

We start with the basic MHD + circuit equations and apply a “resistive timescale ordering”

Introduce small parameter  $\varepsilon \ll 1$

$$\frac{\partial}{\partial t} \sim \mathbf{V} \sim \mathbf{E} \sim V_i \sim \eta \sim R \sim \varepsilon$$

All equations pick up a factor of  $\varepsilon$ , in all terms, which cancels out, except in the momentum equation, where the inertial terms are multiplied by  $\varepsilon^2$ .

To model this “vertical instability” in realistic geometry, and taking the non-rigid motion of the plasma into account, we take advantage of the fact that the unstable mode does not depend on the plasma mass (or inertia), and the stable modes are very high frequency and low amplitude.

$$\frac{\partial \mathbf{B}}{\partial t} = -\nabla \times \mathbf{E}$$

$$\cancel{\varepsilon^2 n M_i \left( \frac{\partial \mathbf{V}}{\partial t} + \mathbf{V} \cdot \nabla \mathbf{V} \right)} + \nabla p = \mathbf{J} \times \mathbf{B} \quad \rightarrow 0$$

$$\mathbf{E} + \mathbf{V} \times \mathbf{B} = \eta \mathbf{J}$$

$$\frac{3}{2} \frac{\partial p}{\partial t} + \nabla \cdot \left( \frac{3}{2} p \mathbf{V} \right) = -p \nabla \cdot \mathbf{V} + \eta J^2$$

$$\mathbf{J} = \nabla \times \mathbf{B}$$

$$\frac{d}{dt} \left[ L_i I_i + \sum_{i \neq j} M_{ij} I_j + \int_P J_\phi G(R_i, R) dR \right] + R_i I_i = V_i$$

We start with the basic MHD + circuit equations and apply a “resistive timescale ordering”

Introduce small parameter  $\varepsilon \ll 1$

$$\frac{\partial}{\partial t} \sim \mathbf{V} \sim \mathbf{E} \sim V_i \sim \eta \sim R \sim \varepsilon$$

This allows us to drop the inertial terms in the momentum equation, and replace it with the equilibrium equation.

Huge simplification....  
removes Alfvén timescale 14

To model this “vertical instability” in realistic geometry, and taking the non-rigid motion of the plasma into account, we take advantage of the fact that the unstable mode does not depend on the plasma mass (or inertia), and the stable modes are very high frequency and low amplitude.

$$\frac{\partial \mathbf{B}}{\partial t} = -\nabla \times \mathbf{E}$$

$$\nabla p = \mathbf{J} \times \mathbf{B}$$

$$\mathbf{E} + \mathbf{V} \times \mathbf{B} = \eta \mathbf{J}$$

$$\frac{3}{2} \frac{\partial p}{\partial t} + \nabla \cdot \left( \frac{3}{2} p \mathbf{V} \right) = -p \nabla \cdot \mathbf{V} + \eta J^2$$

$$\mathbf{J} = \nabla \times \mathbf{B}$$

$$\frac{d}{dt} \left[ L_i I_i + \sum_{i \neq j} M_{ij} I_j + \int_P J_\phi G(R_i, R) dR \right] + R_i I_i = V_i$$

## Grad-Hogan Method

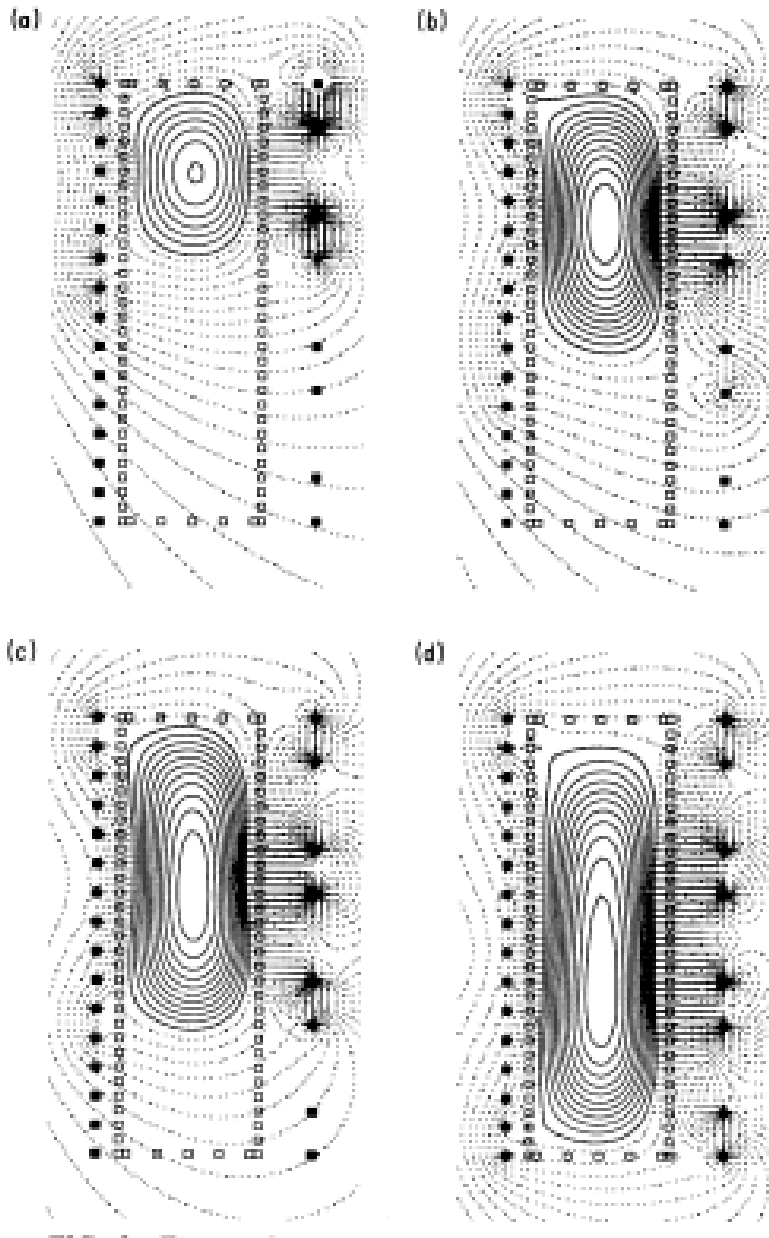
H. Grad and J. Hogan, PRL, 24 1337 (1970)

This is the set of equations we solve to simulate control of the plasma position and shape.

There are 3 production codes that solve these nonlinear equations in 2D and are used to design and test control strategies.

- TSC<sup>1</sup> (PPPL)
- DINA (Russia)
- CORSICA (LLNL)

<sup>1</sup>Can also be run in a mode with plasma mass



Time sequence of using the TSC code to model the evolution of a highly elongated plasma in the TCV tokamak.

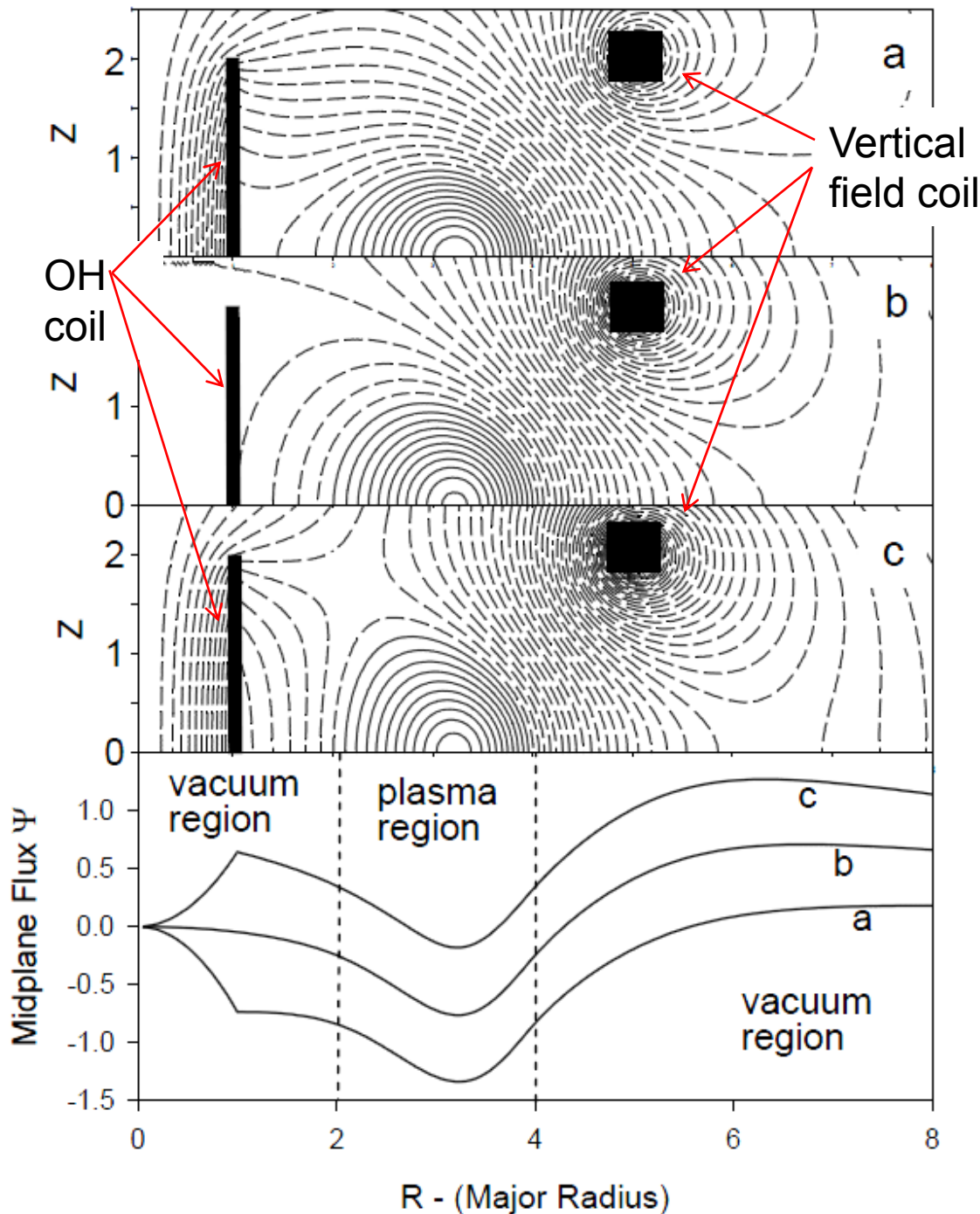
At each instant of time, the vacuum vessel is providing stabilization on the fast (ideal MHD) time scale. The external coils are both feedback stabilizing the plasma and providing shaping fields as they slowly elongate it to fill the entire vessel.

In this case, there were 4 PID feedback systems corresponding to:

- Vertical position
- Radial position
- Elongation
- Squareness

Marcus, Jardin, and Hofmann, PRL, **55** 2289 (1985)





Codes can also accurately model the current drive action of the OH coils.

Simulation of flattop phase of a basic tokamak discharge.

(a) At start of flattop, OH coil has current in same direction as plasma current

(b) Flux in plasma uniformly increases due to resistive dissipation. OH and Vertical field coils adjust boundary values so flux gradient in plasma remains almost unchanged.

$$\mathbf{B}_p = \nabla \phi \times \nabla \Psi$$

(c) At end of flattop, OH coil has current in opposite direction as plasma current.

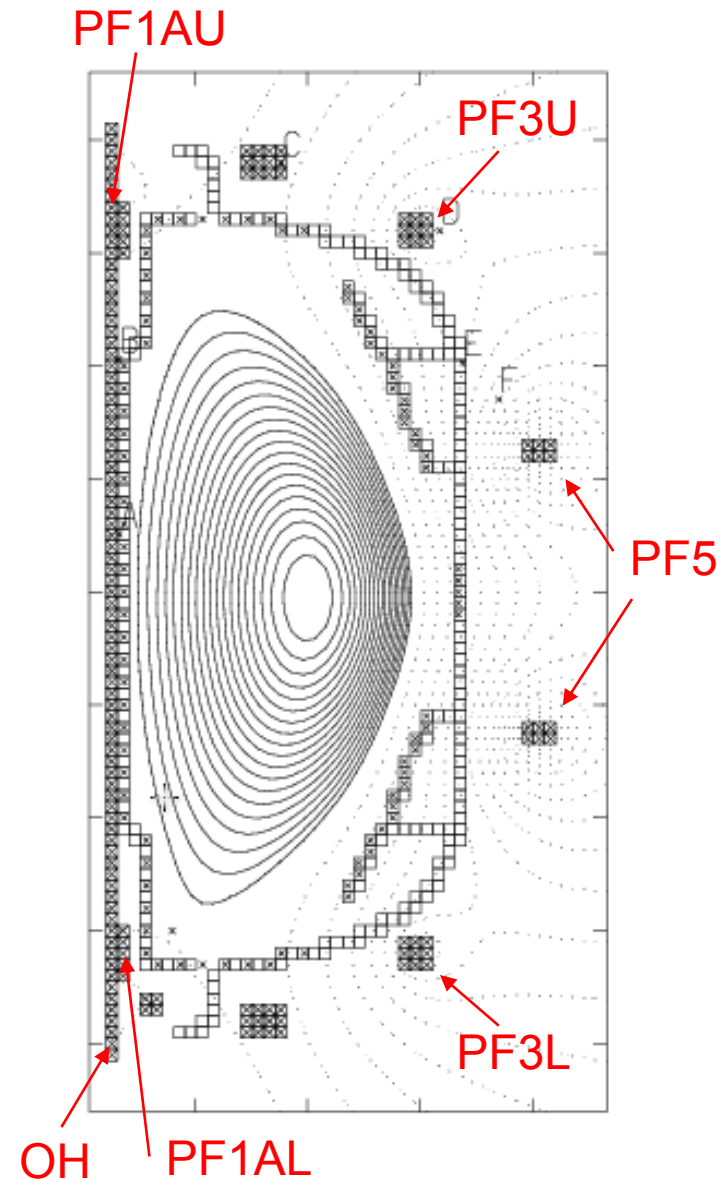
## Simulation of NSTX discharge evolution

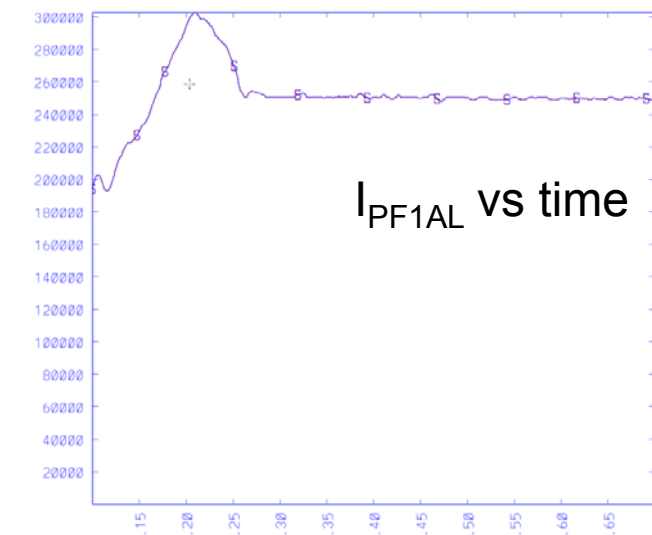
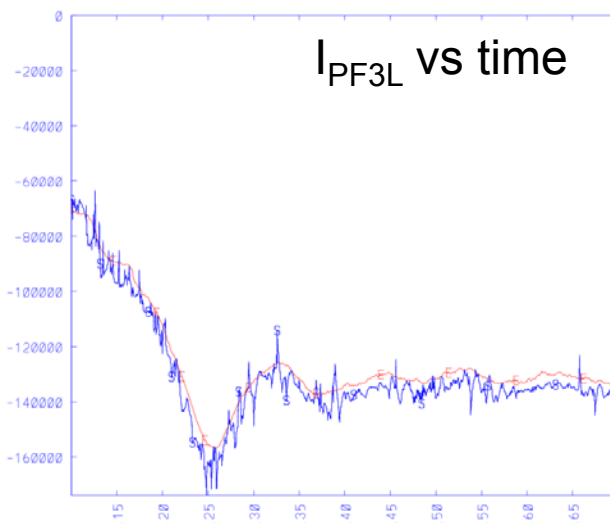
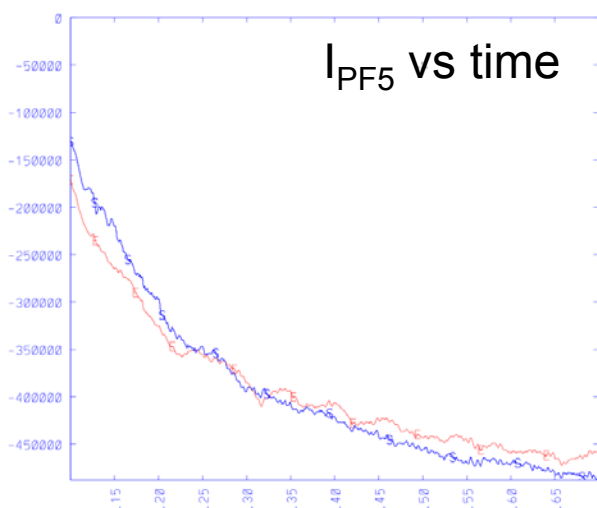
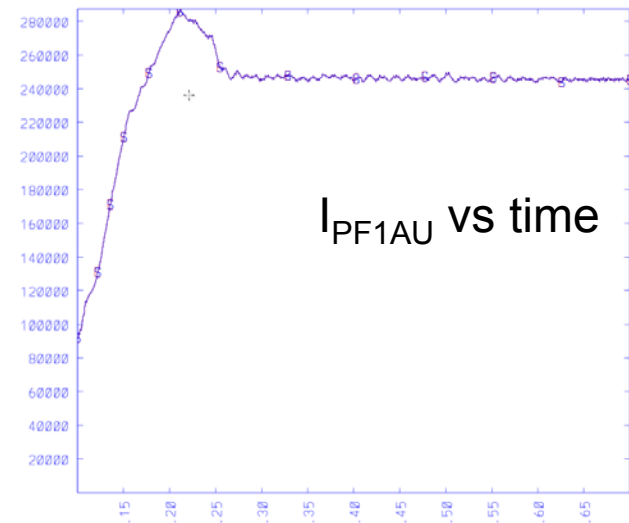
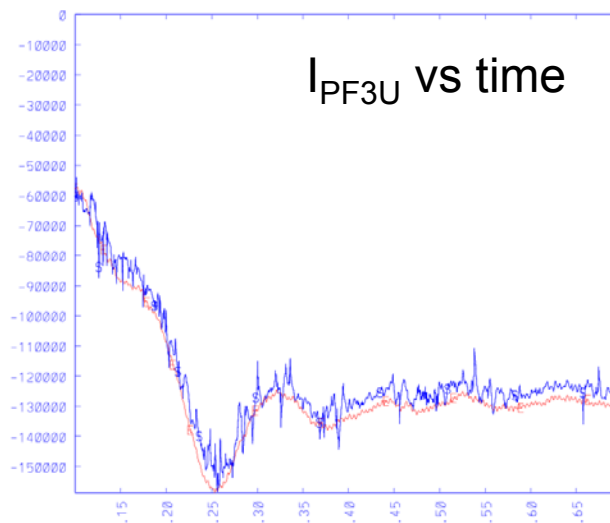
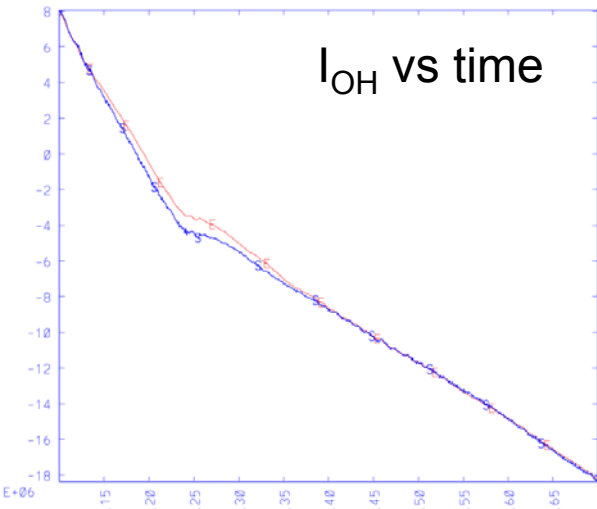
As a validation exercise, we have simulated the evolution of a NSTX discharge using the experimental values of the coil currents as the preprogrammed currents.

$$I_i(t) = I_{PP}(t) + I_{FB}(t)$$

To control the plasma in the simulation, several feedback systems need to be added to the coil groups. The “goodness” of the simulation is measured by how small the current in these feedback systems is to still match other measured quantities (such as the flux in flux loops).

In general, we find that if we can match the plasma density and temperature evolution, then we can predict the plasma current evolution very accurately.



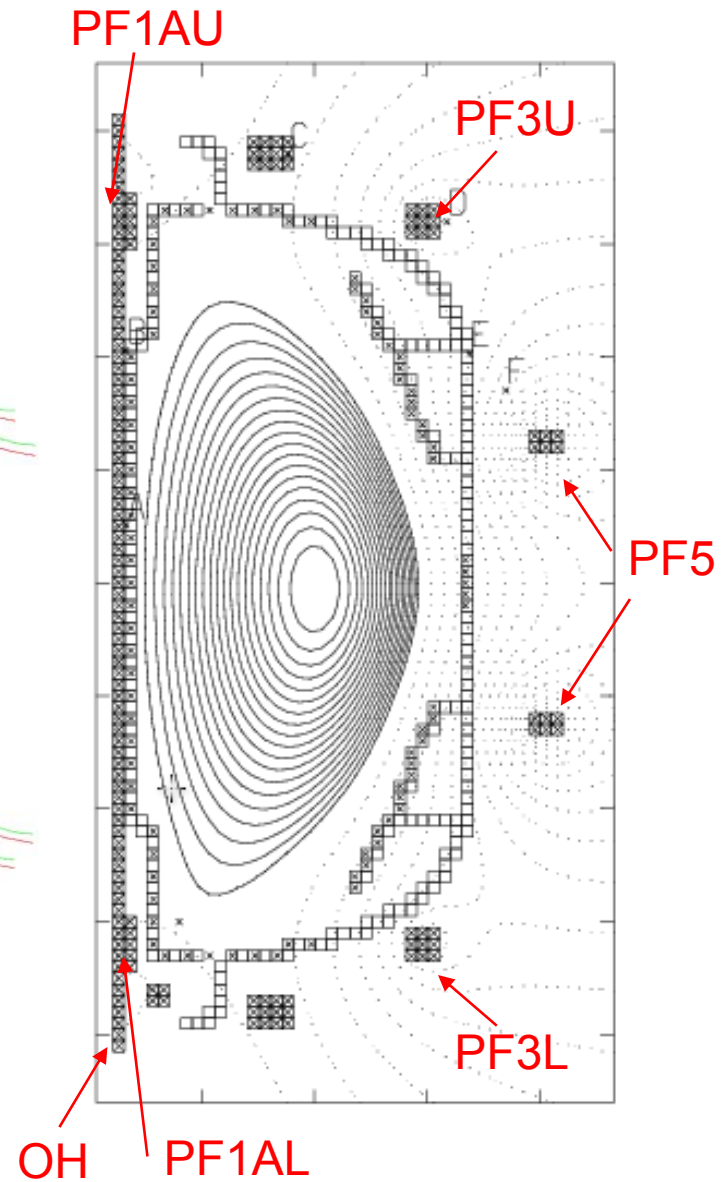
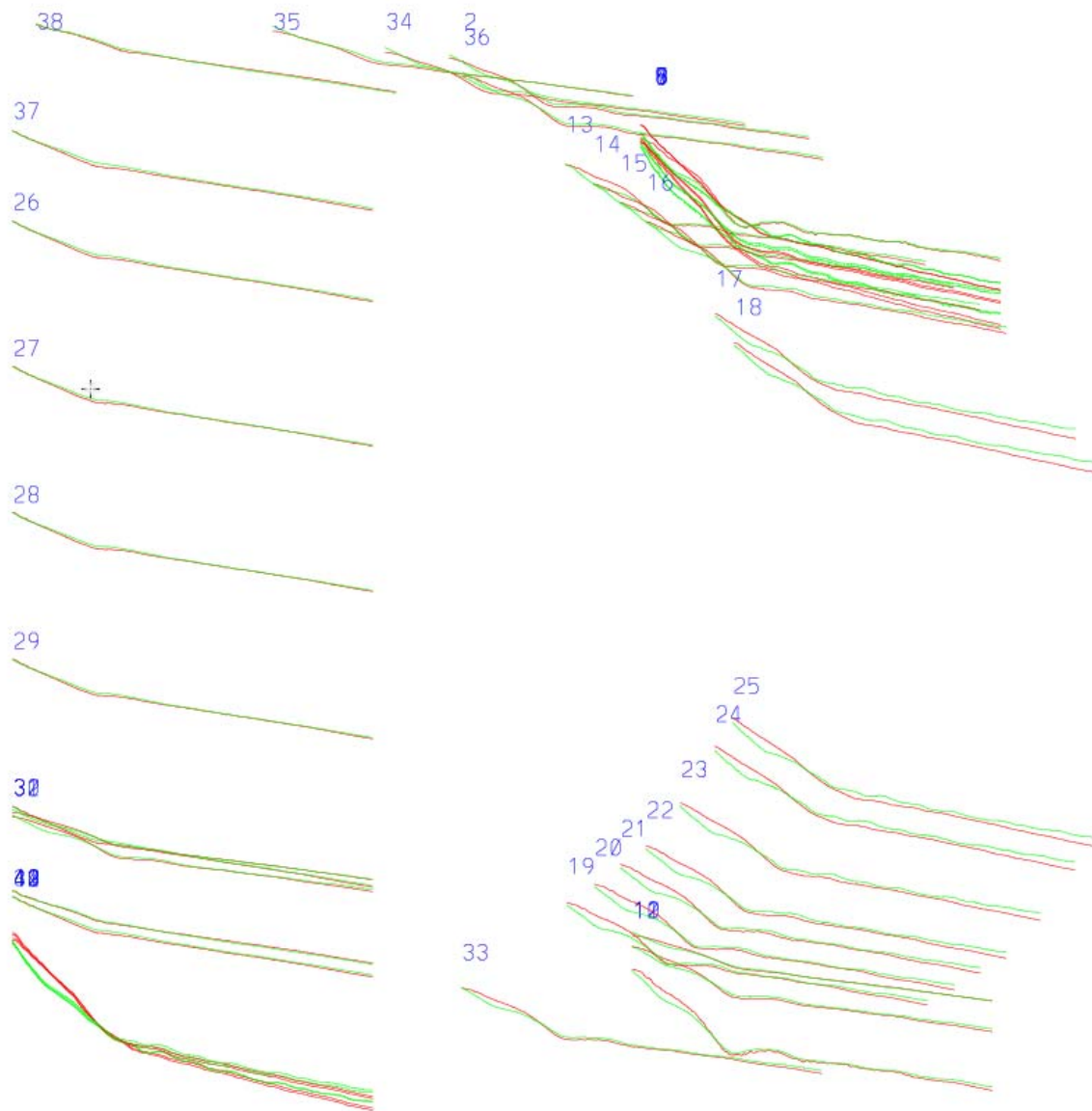


Simulation  $I_{OH}$  has feedback added to match experimental plasma current  $I_P$

Simulation  $I_{PF3U}$  and  $I_{PF3L}$  have vertical stability feedback added

Simulation  $I_{PF5}$  have radial feedback system added

— experiment  
— simulation



Red are simulation flux loop data and green are experimental data. Origin of each curve is approximate position of flux loop around machine.

Excellent agreement!

# Outline

Part I: 2D tokamak instabilities and our ability to predict them with MHD equations

**Part 2:** 3D tokamak instabilities and our ability to predict them with MHD equations

## Summary of Material Presented.

In 2D (axisymmetry) we can use nonlinear MHD codes to accurately model the position, shape control, and current control feedback systems in tokamaks, and these codes are routinely used in the design and optimization of all tokamaks ....including ITER.

The next question is: **How effective can similar codes be for 3D instabilities?**

We have a SciDAC<sup>1</sup> center devoted to answering this question.

<sup>1</sup>Scientific Discovery through Advanced Computing

# Center for Extended MHD Modeling

S. Jardin PI  
2001-2010

**GA:** V. Izzo, N. Ferraro

**U. Washington:** A. Glasser, C. Kim

**MIT:** L. Sugiyama, J. Ramos

**NYU:** H. Strauss

**PPPL:** J. Breslau, M. Chance, J. Chen, S. Hudson

**TechX:** S. Kruger, T. Jenkins, A. Pletzer

**U. Colorado:** S. Parker

**U. Wisconsin:** C. Sovinec, D. Schnack

**Utah State:** E. Held

*a SciDAC activity...*  
*Partners with:*  
TOPS  
ITAPS  
APDEC  
SWIM  
CPES

**NIMROD** and **M3D** codes  
(+ new code development  
such as **M3D-C<sup>1</sup>** code)



# 3D 2-Fluid MHD Equations in a Magnetized Torus:

$$\frac{\partial n}{\partial t} + \nabla \cdot (n\mathbf{V}) = 0$$

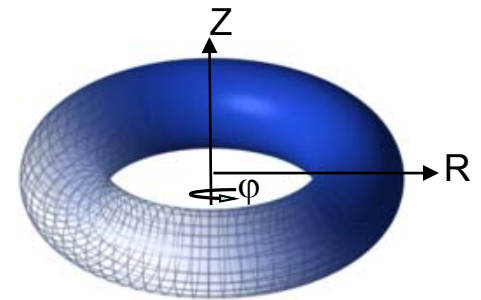
$$\frac{\partial \mathbf{B}}{\partial t} = -\nabla \times \mathbf{E} \quad \mathbf{B} = \nabla \times \mathbf{A} \quad \mathbf{J} = \nabla \times \mathbf{B}$$

$$nM_i \left( \frac{\partial \mathbf{V}}{\partial t} + \mathbf{V} \cdot \nabla \mathbf{V} \right) + \nabla p = \mathbf{J} \times \mathbf{B} - \nabla \cdot \mathbf{\Pi}_{GV} + \mu \nabla^2 \mathbf{V}$$

$$\mathbf{E} + \mathbf{V} \times \mathbf{B} = \eta \mathbf{J} + \frac{1}{ne} (\mathbf{J} \times \mathbf{B} - \nabla p_e) - \lambda_H \nabla^2 \mathbf{J}$$

$$\frac{3}{2} \frac{\partial p_e}{\partial t} + \nabla \cdot \left( \frac{3}{2} p_e \mathbf{V} \right) = -p_e \nabla \cdot \mathbf{V} + \eta J^2 + \frac{\mathbf{J}}{ne} \cdot \left[ \frac{3}{2} \nabla p_e - \frac{5}{2} \frac{p_e}{n} \nabla n \right] - \nabla \cdot \mathbf{q}_e + Q_\Delta$$

$$\frac{3}{2} \frac{\partial p_i}{\partial t} + \nabla \cdot \left( \frac{3}{2} p_i \mathbf{V} \right) = -p_i \nabla \cdot \mathbf{V} + \mu |\nabla V|^2 - \nabla \cdot \mathbf{q}_i - Q_\Delta$$



Resistive MHD  
2-fluid terms

No further approximations!  
Solve these as faithfully as  
possible in realistic geometry

In 3D, we cannot generally  
ignore inertial terms. Very  
stiff system of equations



# 3D 2-Fluid MHD Equations in a Magnetized Torus:

$$\frac{\partial n}{\partial t} + \nabla \cdot (n\mathbf{V}) = 0$$

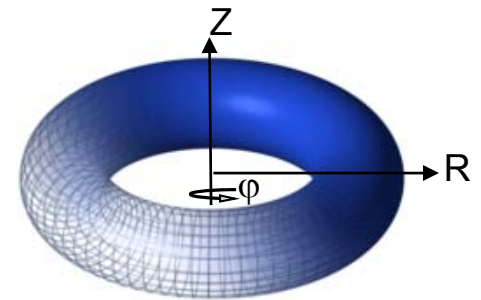
$$\frac{\partial \mathbf{B}}{\partial t} = -\nabla \times \mathbf{E} \quad \mathbf{B} = \nabla \times \mathbf{A} \quad \mathbf{J} = \nabla \times \mathbf{B}$$

$$nM_i \left( \frac{\partial \mathbf{V}}{\partial t} + \mathbf{V} \cdot \nabla \mathbf{V} \right) + \nabla p = \mathbf{J} \times \mathbf{B} - \nabla \cdot \mathbf{\Pi}_{GV} + \mu \nabla^2 \mathbf{V}$$

$$\mathbf{E} + \mathbf{V} \times \mathbf{B} = \eta \mathbf{J} + \frac{1}{ne} (\mathbf{J} \times \mathbf{B} - \nabla p_e) - \lambda_H \nabla^2 \mathbf{J}$$

$$\frac{3}{2} \frac{\partial p_e}{\partial t} + \nabla \cdot \left( \frac{3}{2} p_e \mathbf{V} \right) = -p_e \nabla \cdot \mathbf{V} + \eta J^2 + \frac{\mathbf{J}}{ne} \cdot \left[ \frac{3}{2} \nabla p_e - \frac{5}{2} \frac{p_e}{n} \nabla n \right] - \nabla \cdot \mathbf{q}_e + Q_\Delta$$

$$\frac{3}{2} \frac{\partial p_i}{\partial t} + \nabla \cdot \left( \frac{3}{2} p_i \mathbf{V} \right) = -p_i \nabla \cdot \mathbf{V} + \mu |\nabla V|^2 - \nabla \cdot \mathbf{q}_i - Q_\Delta$$



Resistive MHD  
2-fluid terms

No further approximations!  
Solve these as faithfully as  
possible in realistic geometry

In 3D, we cannot generally  
ignore inertial terms. Very  
stiff system of equations  
=> implicit methods

# Implicit Methods for Wave Equations-1

Consider the model  
wave equation:

$$V(x, t)$$

$$p(x, t)$$

$$\frac{\partial V}{\partial t} = \frac{\partial p}{\partial x}$$

$$\frac{\partial p}{\partial t} = c_s^2 \frac{\partial V}{\partial x}$$

$\delta x$  zone size

$\delta t$  time step

$$V_j^n \equiv V(j\delta x, n\delta t)$$

In order to solve this with a large stable time step, we must evaluate the spatial derivatives at the advanced time

$$V_j^{n+1} = V_j^n + \frac{\delta t}{\delta x} \left[ p_{j+1/2}^{n+1} - p_{j-1/2}^{n+1} \right]$$

$$p_{j+1/2}^{n+1} = p_{j+1/2}^n + c_s^2 \frac{\delta t}{\delta x} \left[ V_{j+1}^{n+1} - V_j^{n+1} \right]$$

This gives a numerically stable scheme for any value of the time step  $\delta t$ . If the spatial derivatives were evaluated at the old time levels, the time step would be limited by the Courant condition:

$$\delta t < \frac{\delta x}{c_s}$$

Way too restrictive!

# Implicit Methods for Wave Equations-2

$$V_j^{n+1} = V_j^n + \frac{\delta t}{\delta x} [p_{j+1/2}^{n+1} - p_{j-1/2}^{n+1}]$$

$$p_{j+1/2}^{n+1} = p_{j+1/2}^n + c_s^2 \frac{\delta t}{\delta x} [V_{j+1}^{n+1} - V_j^{n+1}]$$

Use the second equation to eliminate the advanced time p from the first equation.

There is a technique now used by most of the major 3D codes for solving this system efficiently.

$$p_{j+1/2}^{n+1} = p_{j+1/2}^n + c_s^2 \frac{\delta t}{\delta x} [V_{j+1}^{n+1} - V_j^{n+1}]$$

$$p_{j-1/2}^{n+1} = p_{j-1/2}^n + c_s^2 \frac{\delta t}{\delta x} [V_j^{n+1} - V_{j-1}^{n+1}]$$

$$V_j^{n+1} - c_s^2 \left( \frac{\delta t}{\delta x} \right)^2 [V_{j+1}^{n+1} - 2V_j^{n+1} + V_{j-1}^{n+1}] = V_j^n + \frac{\delta t}{\delta x} [p_{j+1/2}^n - p_{j-1/2}^n]$$

$$p_{j+1/2}^{n+1} = p_{j+1/2}^n + c_s^2 \frac{\delta t}{\delta x} [V_{j+1}^{n+1} - V_j^{n+1}]$$

# Implicit Methods for Wave Equations-3

$$V_j^{n+1} - c_s^2 \left( \frac{\delta t}{\delta x} \right)^2 \left[ V_{j+1}^{n+1} - 2V_j^{n+1} + V_{j-1}^{n+1} \right] = V_j^n + \frac{\delta t}{\delta x} \left[ p_{j+1/2}^n - p_{j-1/2}^n \right]$$

$$p_{j+1/2}^{n+1} = p_{j+1/2}^n + c_s^2 \frac{\delta t}{\delta x} \left[ V_{j+1}^{n+1} - V_j^{n+1} \right]$$

Define the second derivative operator:  $\frac{\partial^2}{\partial x^2} V_j^{n+1} \equiv \left( \frac{1}{\delta x} \right)^2 \left[ V_{j+1}^{n+1} - 2V_j^{n+1} + V_{j-1}^{n+1} \right]$

The implicit algorithm for the wave equation can then be written as:

Well conditioned, diagonally dominant operator.  $\longrightarrow$   $\left( 1 - c_s^2 \delta t^2 \frac{\partial^2}{\partial x^2} \right) V_j^{n+1} = V_j^n + \frac{\delta t}{\delta x} \left[ p_{j+1/2}^n - p_{j-1/2}^n \right]$

These two equations can be solved sequentially!  $p_{j+1/2}^{n+1} = p_{j+1/2}^n + c_s^2 \frac{\delta t}{\delta x} \left[ V_{j+1}^{n+1} - V_j^{n+1} \right]$

## Implicit Methods for Wave Equations-4

$$\begin{aligned} \frac{\partial V}{\partial t} &= \frac{\partial p}{\partial x} \\ \frac{\partial p}{\partial t} &= c_s^2 \frac{\partial V}{\partial x} \end{aligned} \quad \rightarrow \quad \begin{aligned} \left(1 - c_s^2 \delta t^2 \frac{\partial^2}{\partial x^2}\right) V_j^{n+1} &= V_j^n + \delta t \left. \frac{\partial p}{\partial x} \right|^n \\ p_{j+1/2}^{n+1} &= p_{j+1/2}^n + c_s^2 \delta t \left. \frac{\partial V}{\partial x} \right|^{n+1} \end{aligned}$$

Apply this same technique to the 3D MHD equations:

$$\begin{aligned} nM_i \frac{\partial \mathbf{V}}{\partial t} + \nabla p &= \mathbf{J} \times \mathbf{B} \\ \frac{\partial \mathbf{B}}{\partial t} &= \nabla \times [\mathbf{V} \times \mathbf{B} - \eta \mathbf{J}] \\ \frac{3}{2} \frac{\partial p}{\partial t} + \nabla \cdot \left( \frac{3}{2} p \mathbf{V} \right) + p \nabla \cdot \mathbf{V} &= 0 \end{aligned} \quad \rightarrow \quad \begin{aligned} nM_i [1 - \delta t^2 L] \mathbf{V}^{n+1} &= \mathbf{V}^n + \delta t [\mathbf{J} \times \mathbf{B} - \nabla p]^n \\ \mathbf{B}^{n+1} &= \mathbf{B}^n + \delta t \nabla \times [\mathbf{V}^{n+1} \times \mathbf{B} - \eta \mathbf{J}] \\ p^{n+1} &= p^n - \delta t \left[ \nabla \cdot (p \mathbf{V}^{n+1}) + \frac{2}{3} p \nabla \cdot \mathbf{V}^{n+1} \right] \end{aligned}$$

Here,  $L\{\mathbf{V}\} \equiv \nabla \times [\nabla \times (\mathbf{V} \times \mathbf{B})] \times \mathbf{B} + (\nabla \times \mathbf{B}) \times [\nabla \times (\mathbf{V} \times \mathbf{B})] + \nabla \left[ \mathbf{v} \cdot \nabla p + \frac{5}{3} p \nabla \cdot \mathbf{V} \right]$

is the self-adjoint ideal MHD operator

# Accuracy and Spectral Pollution

Because the externally imposed toroidal field in a tokamak is very strong, any plasma instability will slip through this field and not compress it. We need to be able to model this motion very accurately because of the weak forces causing the instability.

In M3D-C<sup>1</sup>, we express the velocity and magnetic fields as shown:  $(R, \phi, Z)$

$$\mathbf{V} = R^2 \nabla \phi \times \nabla U + R^2 \omega \nabla \phi + \frac{1}{R^4} \nabla_{\perp} \chi$$

$$\mathbf{B} = \nabla \psi \times \nabla \phi - \nabla \frac{\partial f}{\partial \phi} + (F_0 + R^2 \nabla^2 f) \nabla \phi$$

Consider now the action of the first term in  $\mathbf{V}$  on the external toroidal field:

$$\mathbf{B} = F_0 \nabla \phi \quad \mathbf{V} = R^2 \nabla \phi \times \nabla U$$

$$\nabla \phi \cdot \left[ \frac{\partial \mathbf{B}}{\partial t} = \nabla \times (\mathbf{V} \times \mathbf{B}) \right]$$

$$\frac{1}{R^2} \frac{\partial F}{\partial t} = \nabla \phi \cdot \nabla \times \left[ \left( R^2 \nabla \phi \times \nabla U \right) \times F_0 \nabla \phi \right]$$

$$= F_0 \nabla \cdot [\nabla U \times \nabla \phi]$$

$$= 0$$



The unstable mode will mostly consist of the velocity component  $U$ .

The velocity field  $U$  does not compress the external toroidal field!

# Status of ELM<sup>1</sup> Calculations

- Recent verification studies have shown that the codes NIMROD and M3D-C<sup>1</sup> can reproduce the stability results of specialized linear ideal-MHD codes in the ideal limit

**ideal limit:**

plasma resistivity  $\rightarrow 0$ .

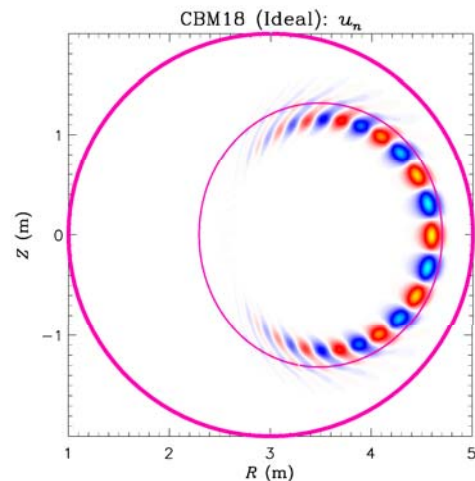
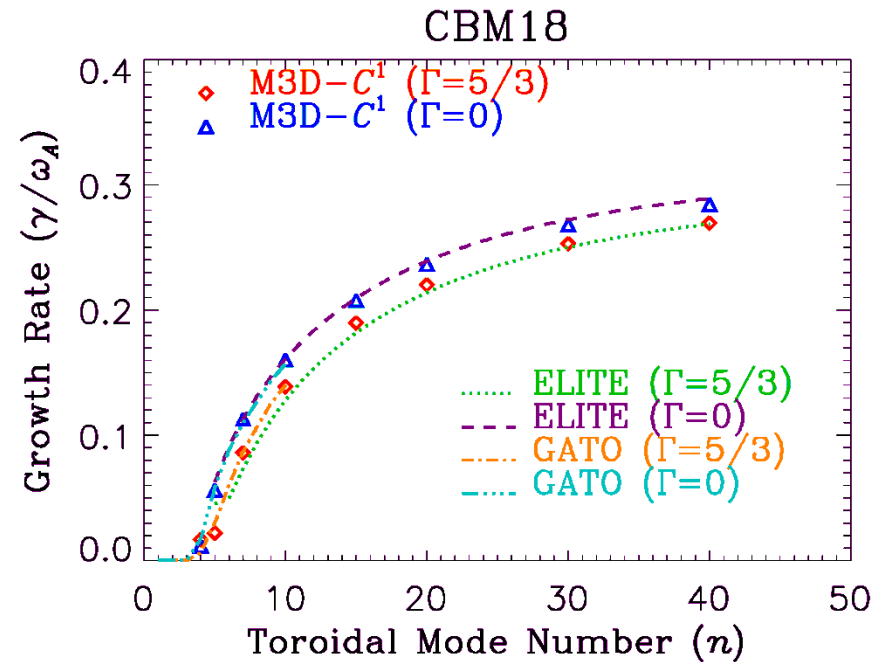
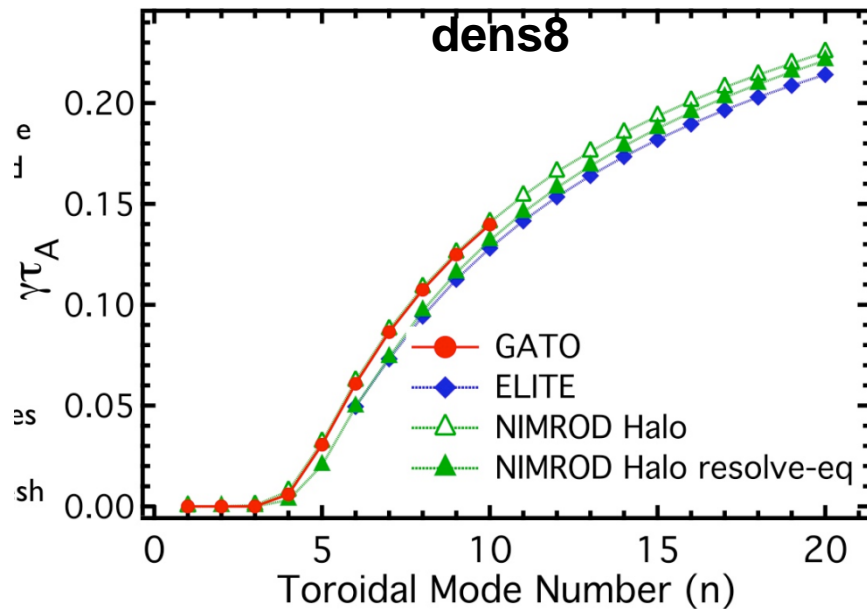
vacuum region resistivity  $\rightarrow \infty$ ,

vacuum region density  $\rightarrow 0$

- Nonlinear ELM simulations with M3D reproduce many experimental signatures of the ELM

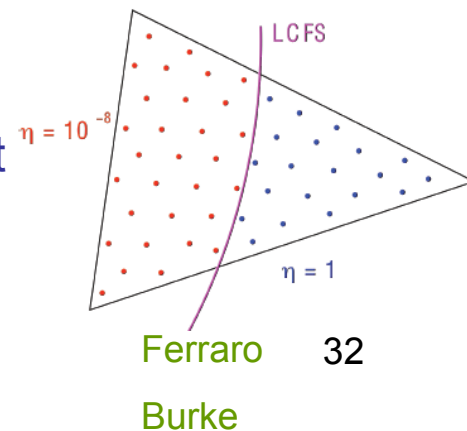
<sup>1</sup>Edge Localized Modes

# Linear ELMs: Code Verification-1



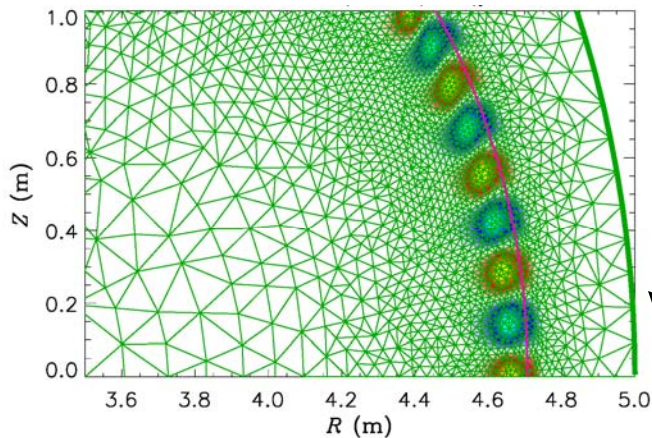
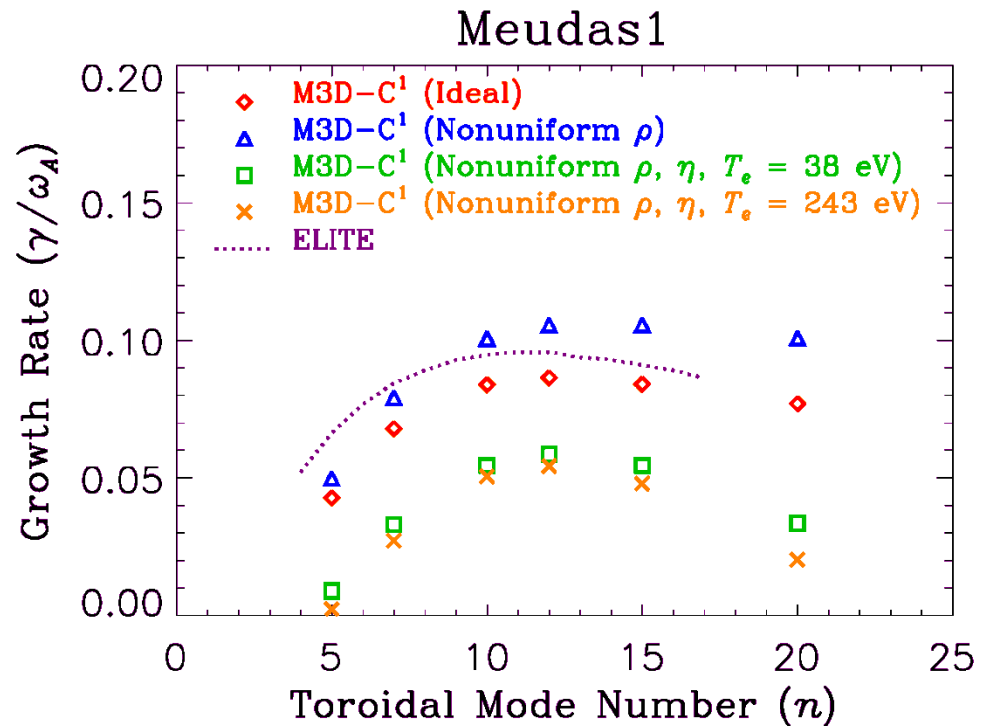
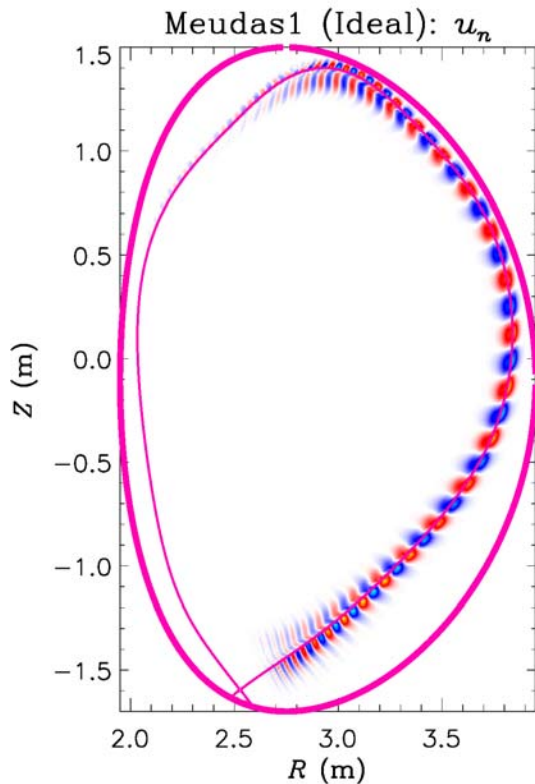
Both **NIMROD** and **M3D-C<sup>1</sup>** have performed detailed benchmarking for ELM unstable equilibrium in the **ideal limit** against GATO and ELITE up to  $n=40$

- required discontinuous  $\eta$  and  $\rho$  profiles with jump of  $10^8$





# Linear ELMs: Code Verification-2



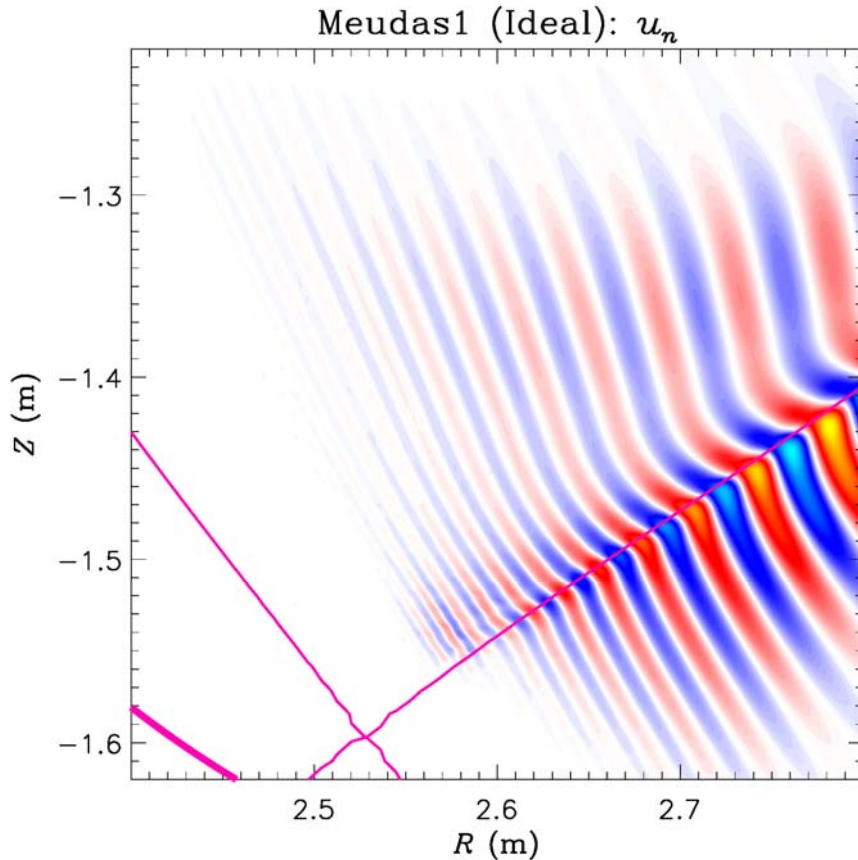
Studies have been extended to:

- diverted equilibrium (JT-60)
- finite resistivity in the plasma and SOL
- realistic density profiles

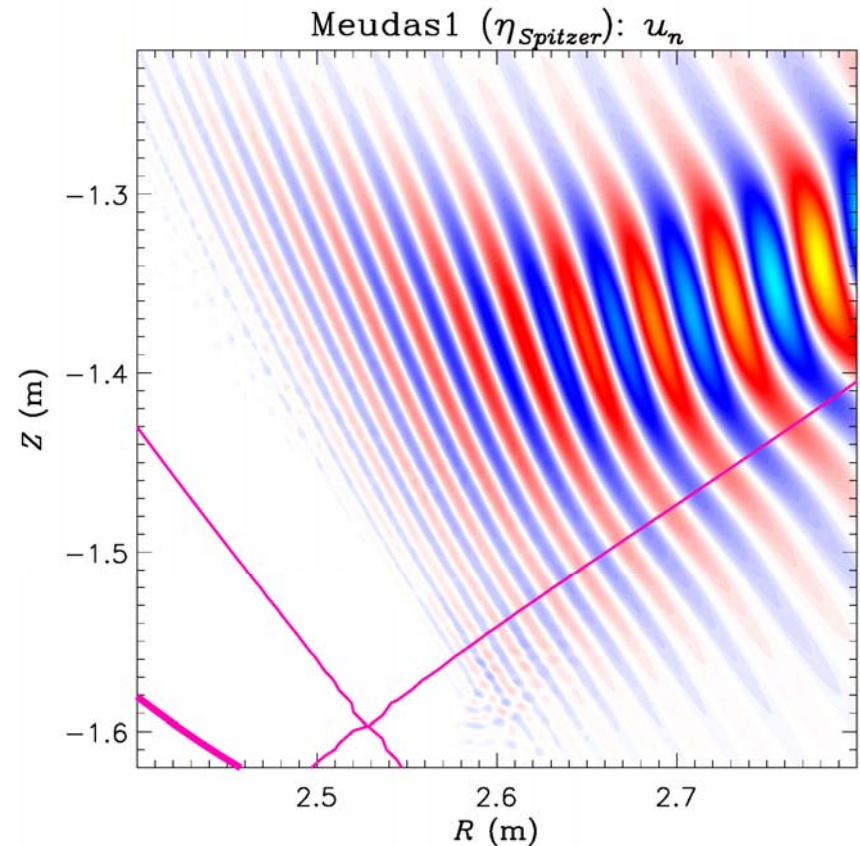
Close-up showing M3D-C<sup>1</sup> triangular adaptive mesh

# Linear ELMs: Code Verification-3

Comparison of eigenfunctions of normal plasma displacement for “ideal limit” and more realistic Spitzer resistivity with SOL with M3D-C<sup>1</sup>



**Ideal MHD limit**

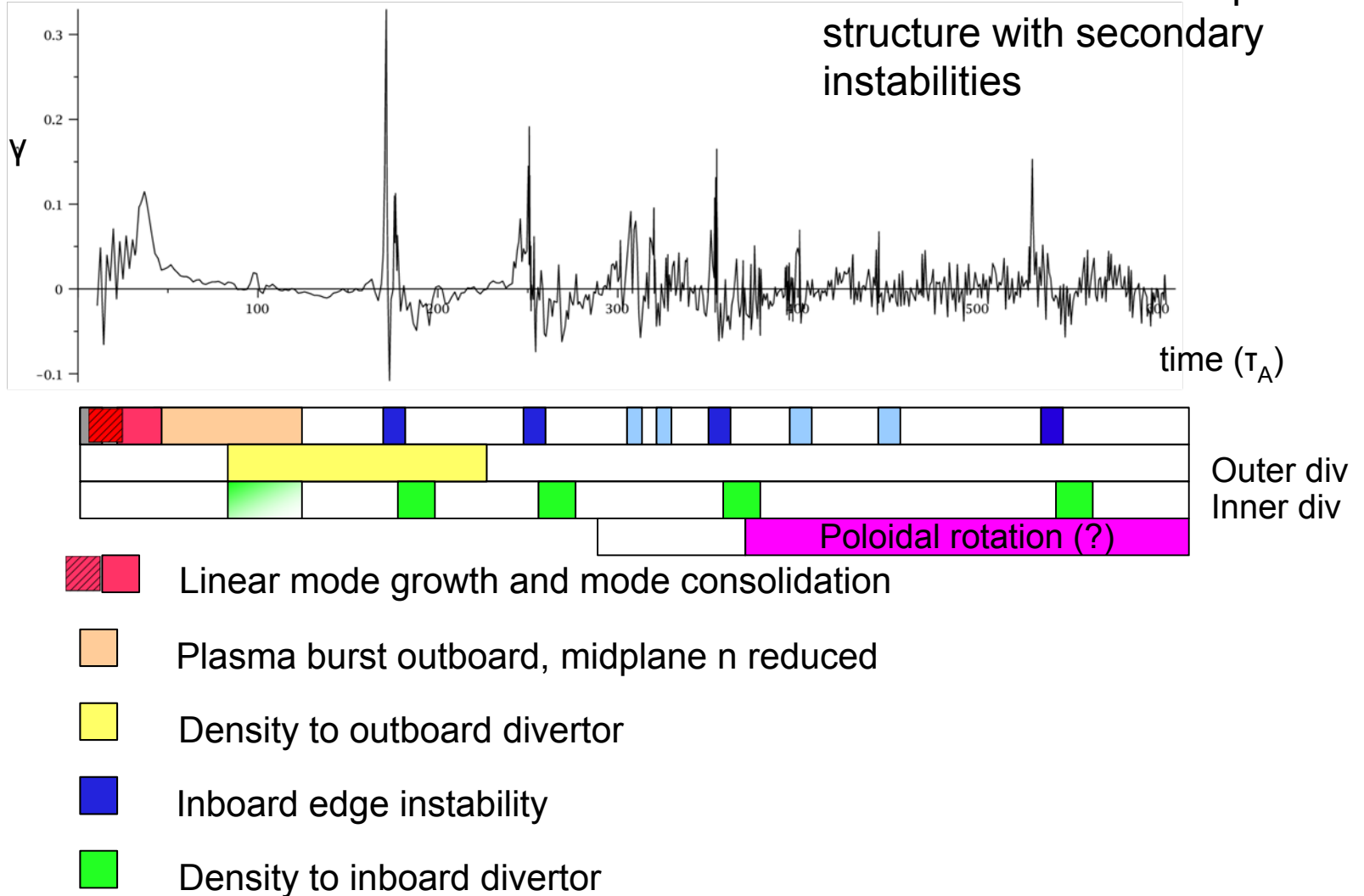


**Spitzer resistivity with SOL**

# Non-linear ELM simulation with M3D

Multi-stage ELM – DIII-D 119690

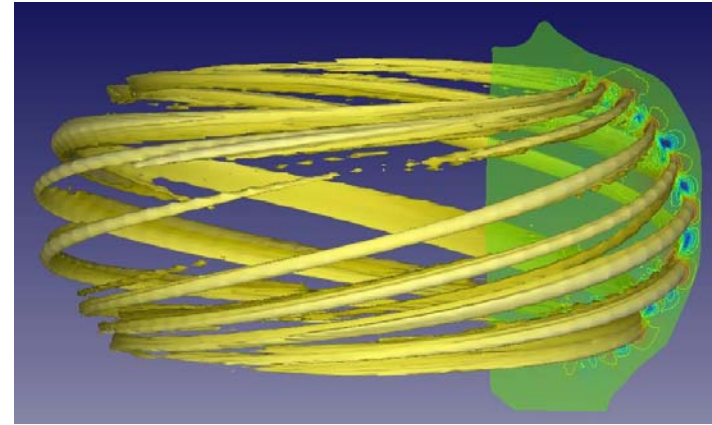
Full simulation of nonlinear ELM event shows complex structure with secondary instabilities



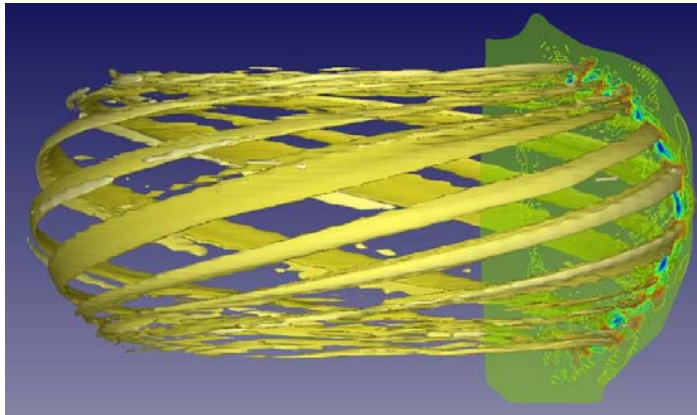
# First 50 $\tau_A$ : linear mode growth Nonlinear harmonic consolidation

Initially many unstable linear modes.  
These rapidly consolidate into lower-n  
field-aligned mode "filaments"  
(n=6-10 at t=43)

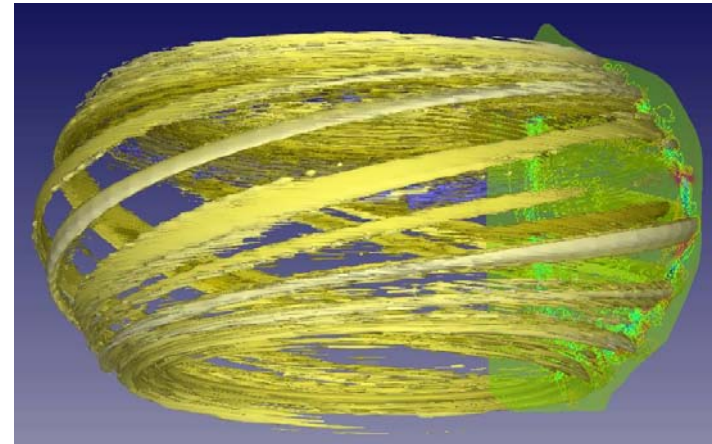
Similar to what is seen experimentally.



$\psi$ -pert



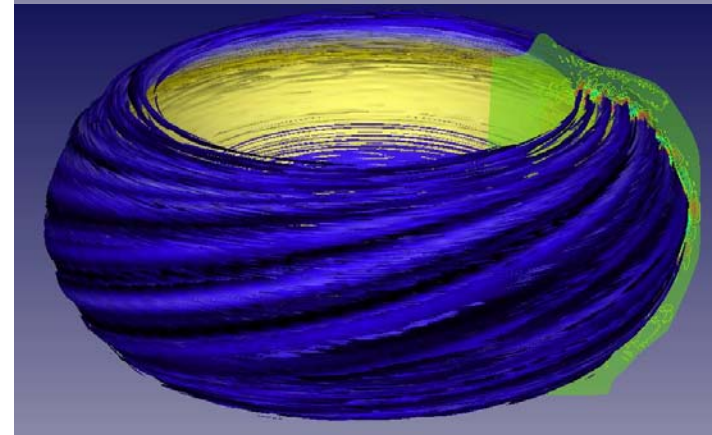
n  
pert



u

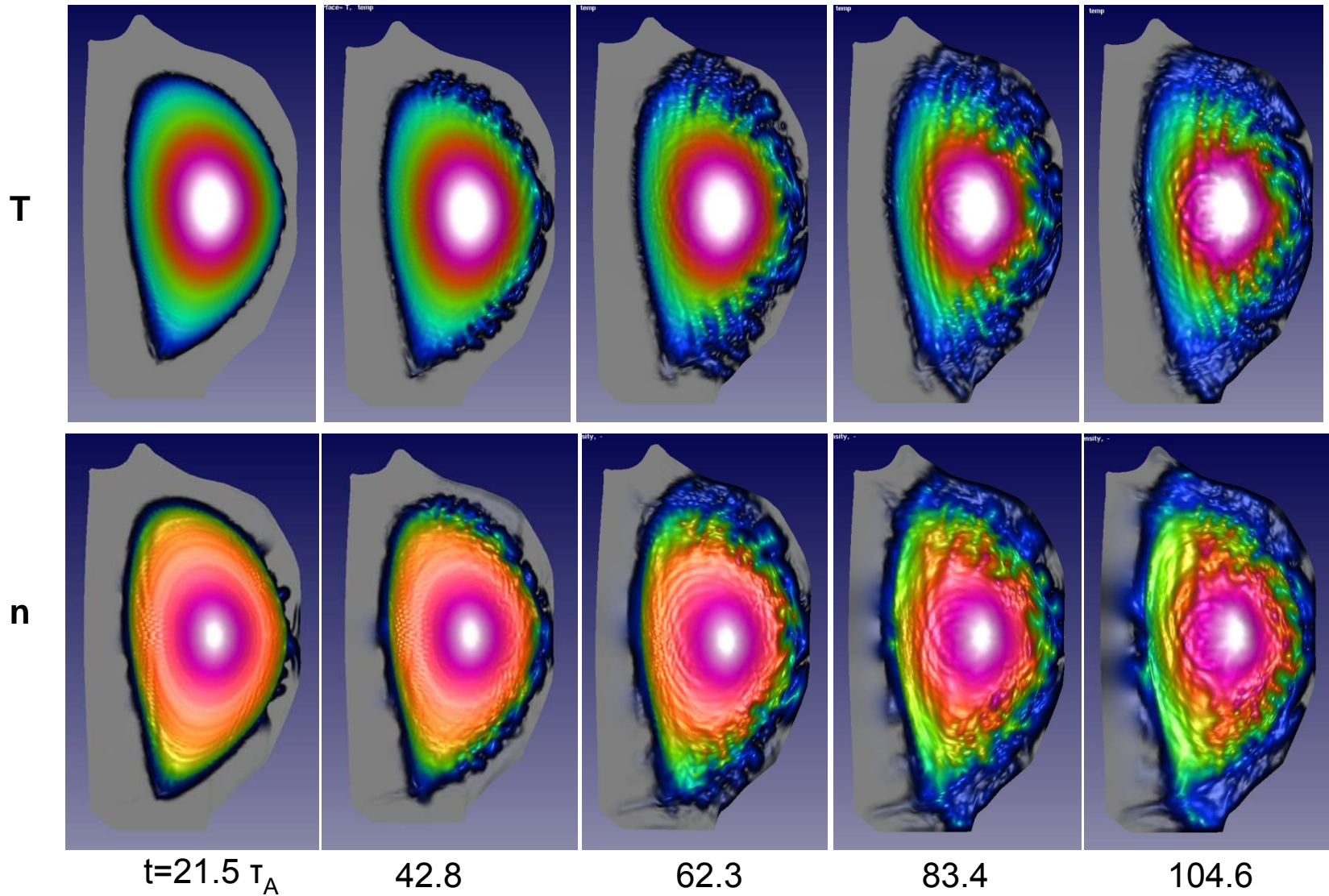


n

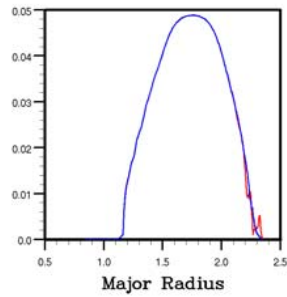
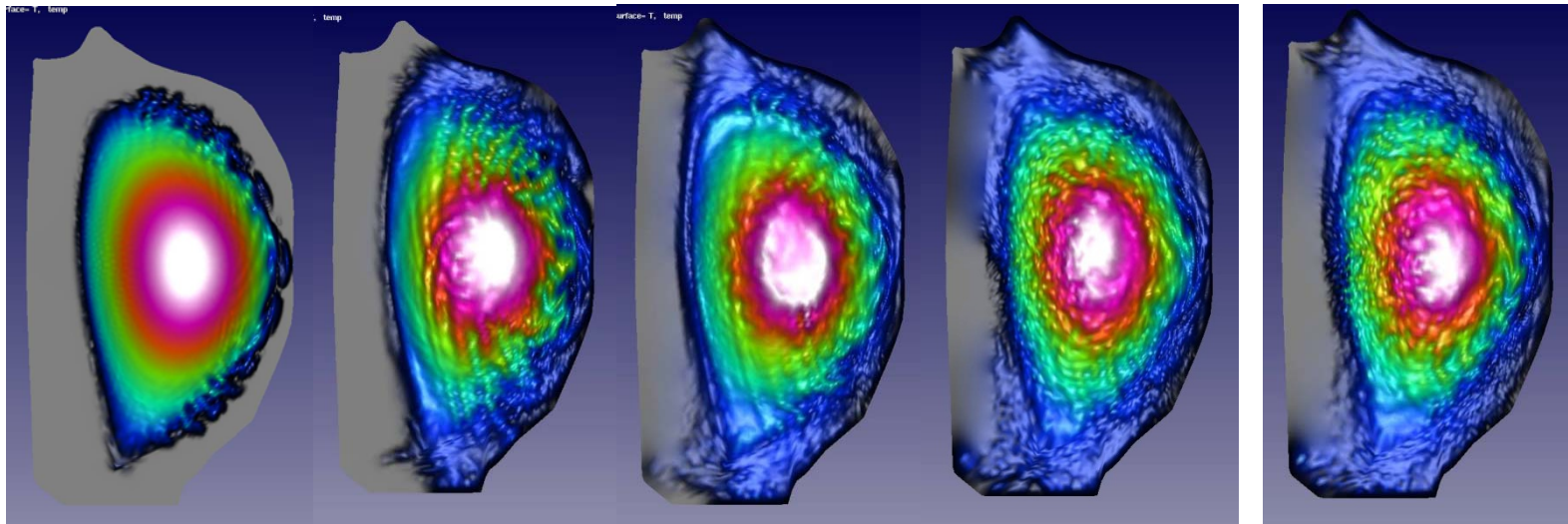


$RJ_\phi$

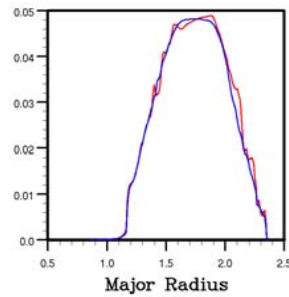
# Early time: T and n ballooning in rapid burst



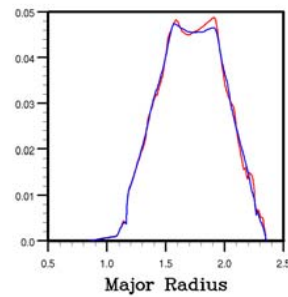
Longer time: T



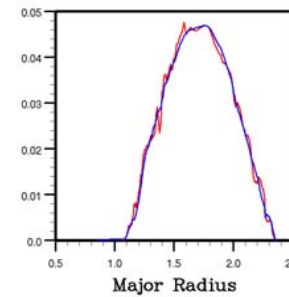
t=43



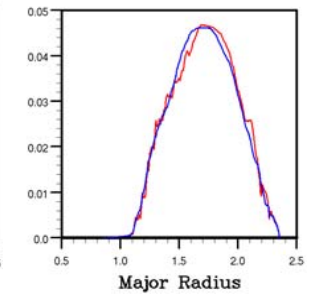
126



227

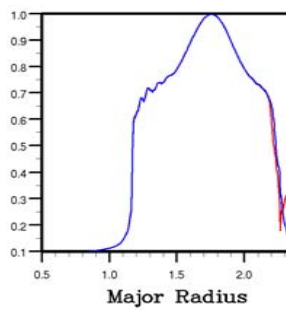
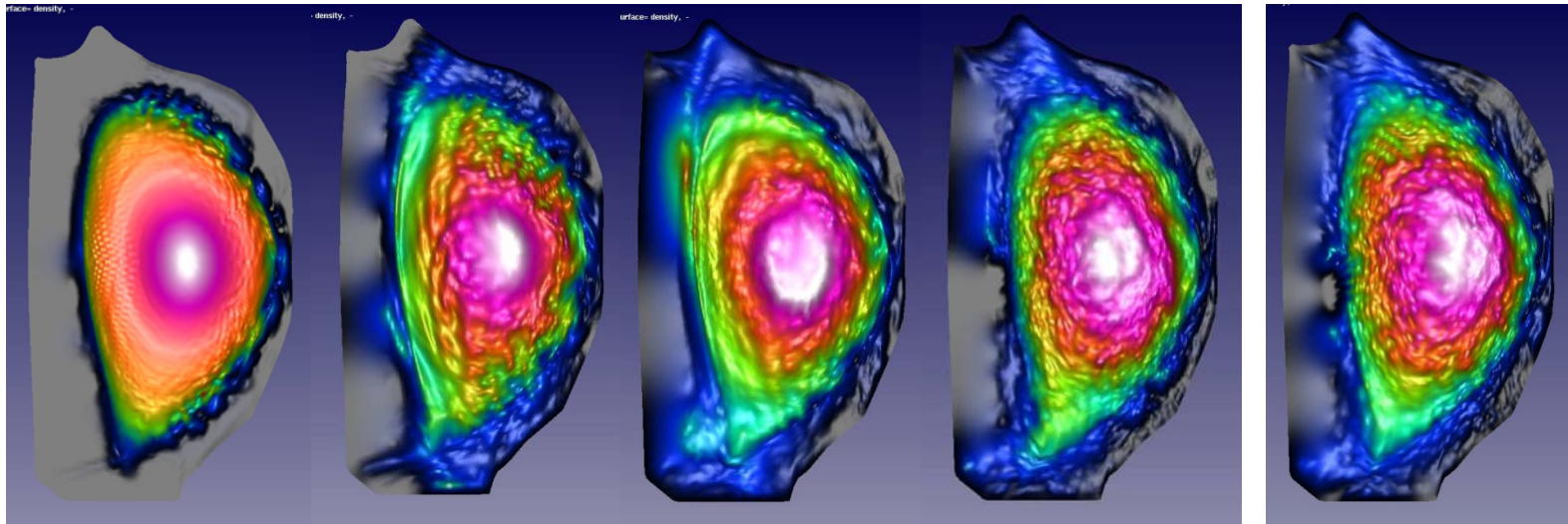


461

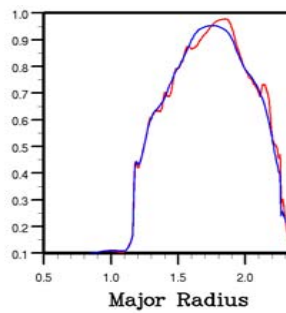


529

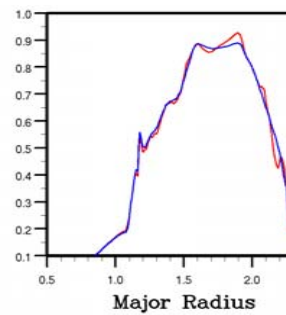
Longer time: n



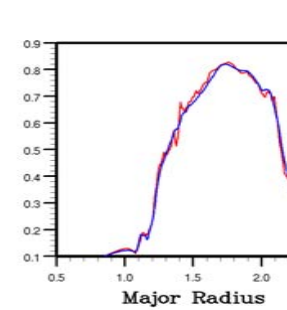
t=43



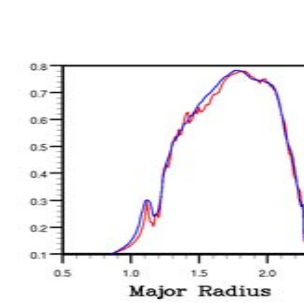
126



227



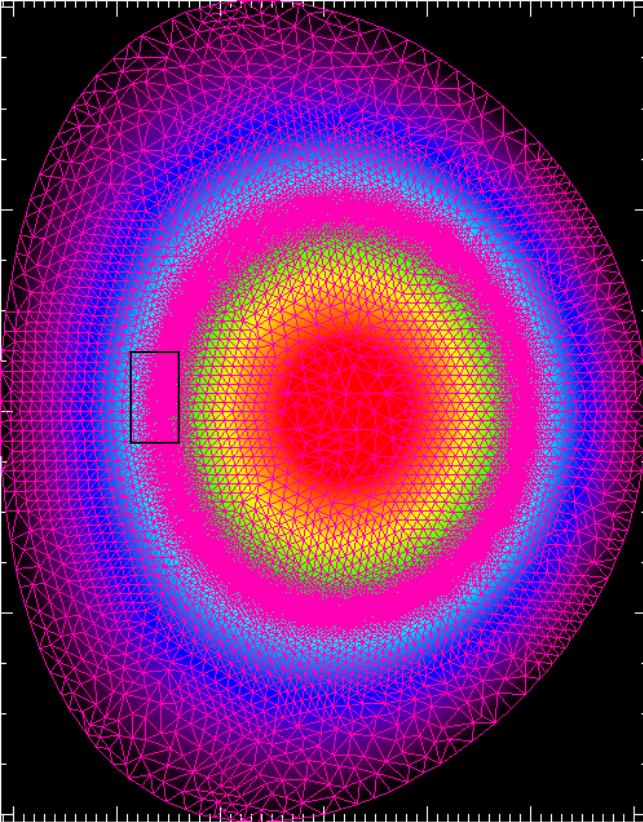
461



529

# High-S tearing mode studies

- M3D- $C^1$ , is now being used for linear physics studies in NSTX, CMOD and ITER
- high order  $C^1$  finite elements, adaptive mesh, and fully implicit time advance allow high resolution studies of localized modes
- Now being used to study tearing (and double tearing) modes at realistic S values, including pressure (Glasser) stabilization

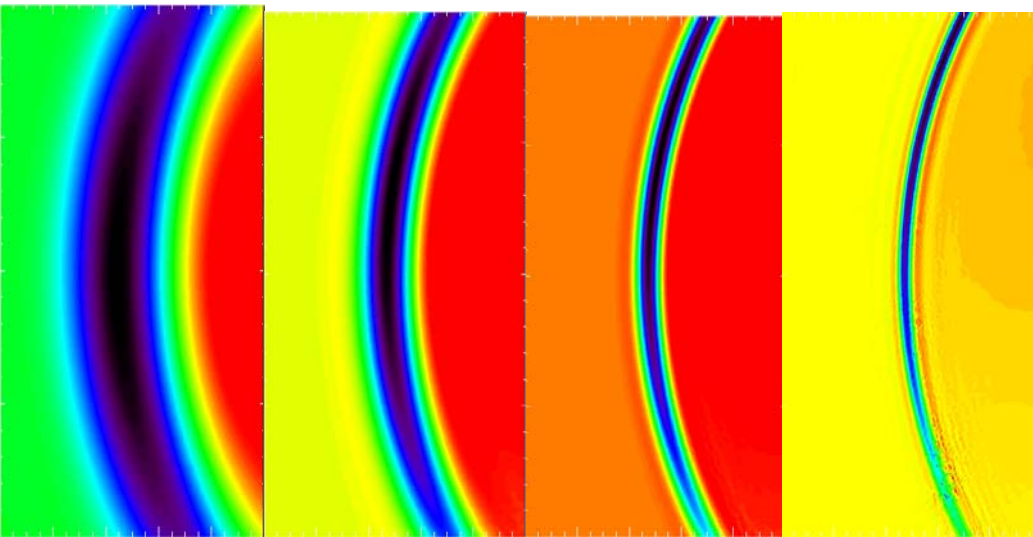


$S=10^5$

$S=10^6$

$S=10^7$

$S=10^8$



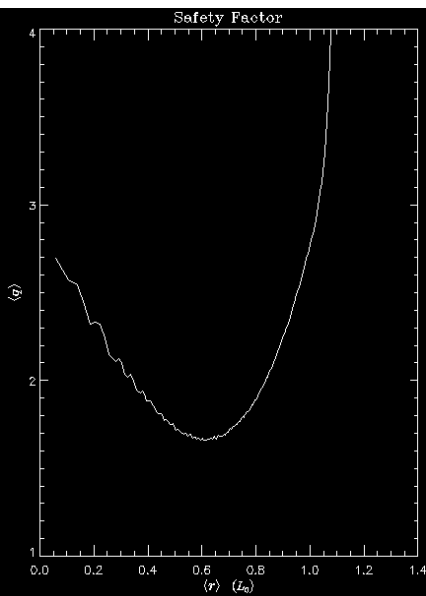
(Top) Equilibrium current density with adaptive mesh superimposed.

(Left) perturbed current density for (1,1) tearing mode at different S. Rightmost figure corresponds to NSTX parameters

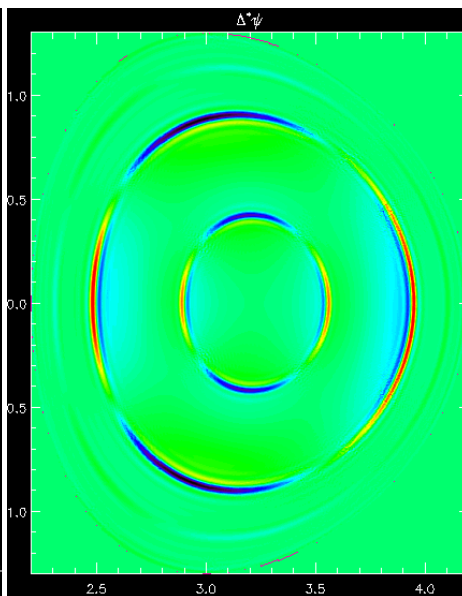


# $n=1$ Double Tearing Mode in NSTX.... $S = 10^8$

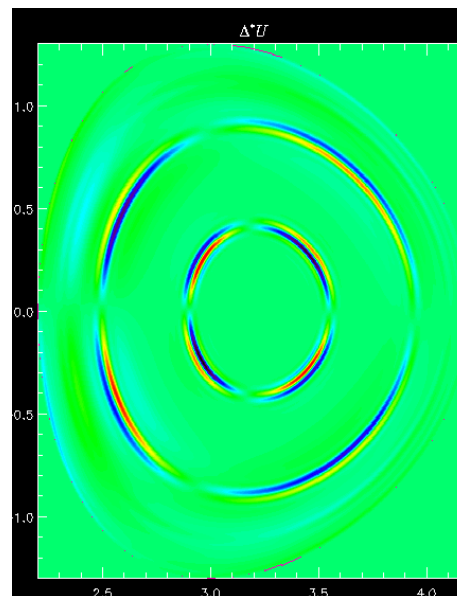
q-profile



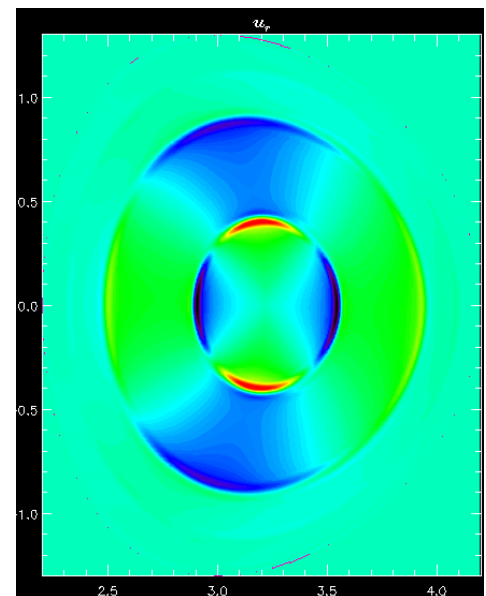
Toroidal current



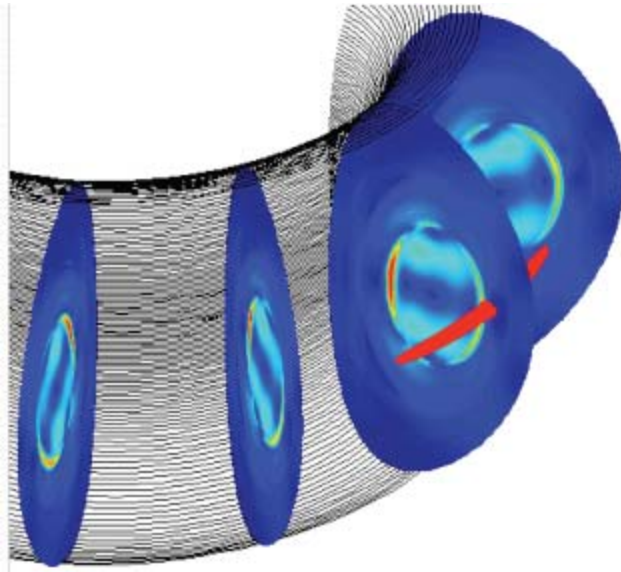
Vorticity



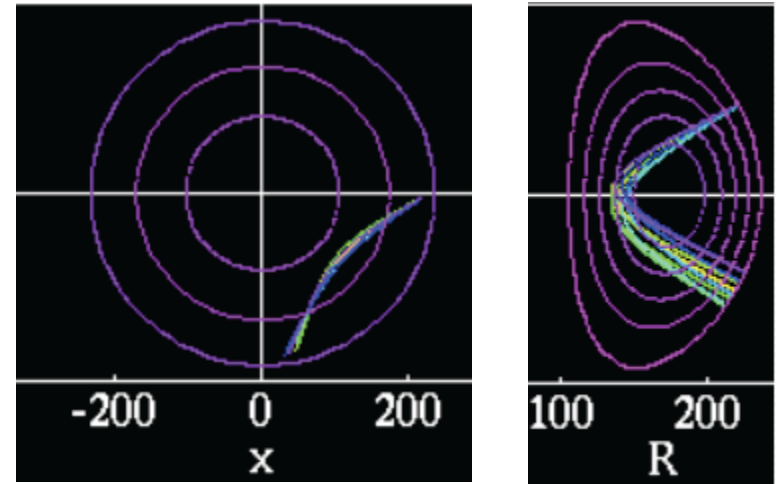
Normal displacement



# ECCD Stabilization of NTM



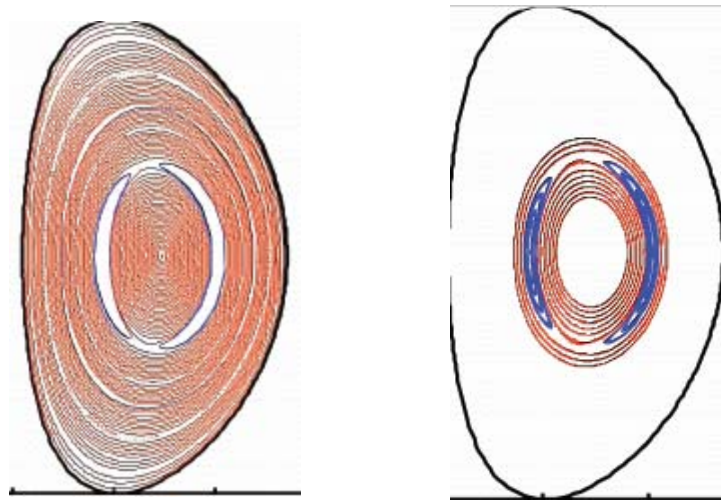
NIMROD code calculates the MHD growth of NTM c



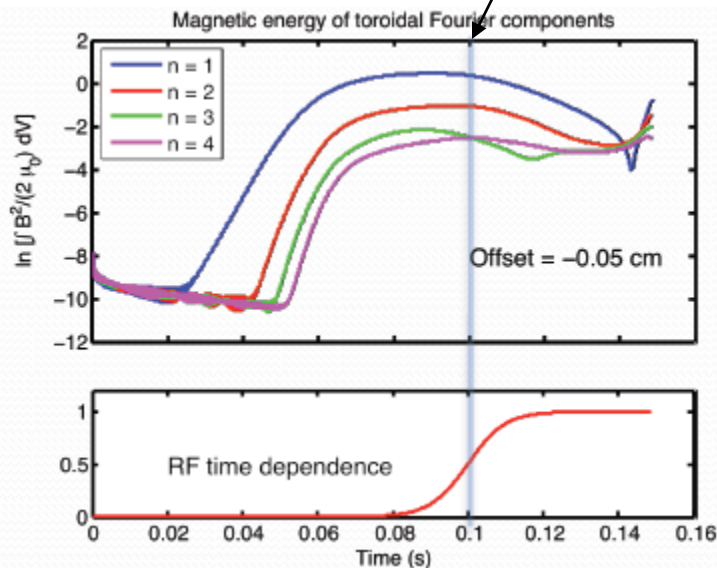
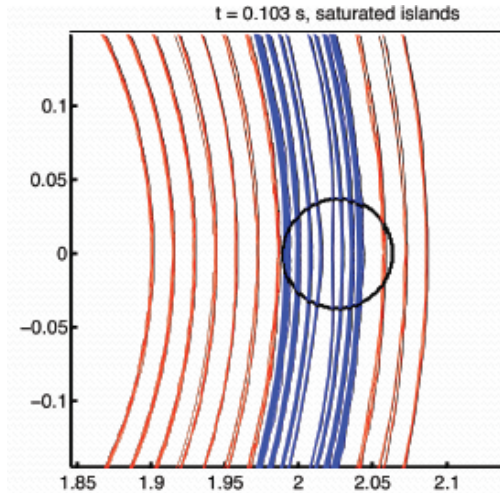
GENRAY code computes wave induced ECCD current drive term

Code coupling provided by SWIM framework

Results to date are for an equilibrium that is tearing unstable and using a model toroidally localized CD term



Close up



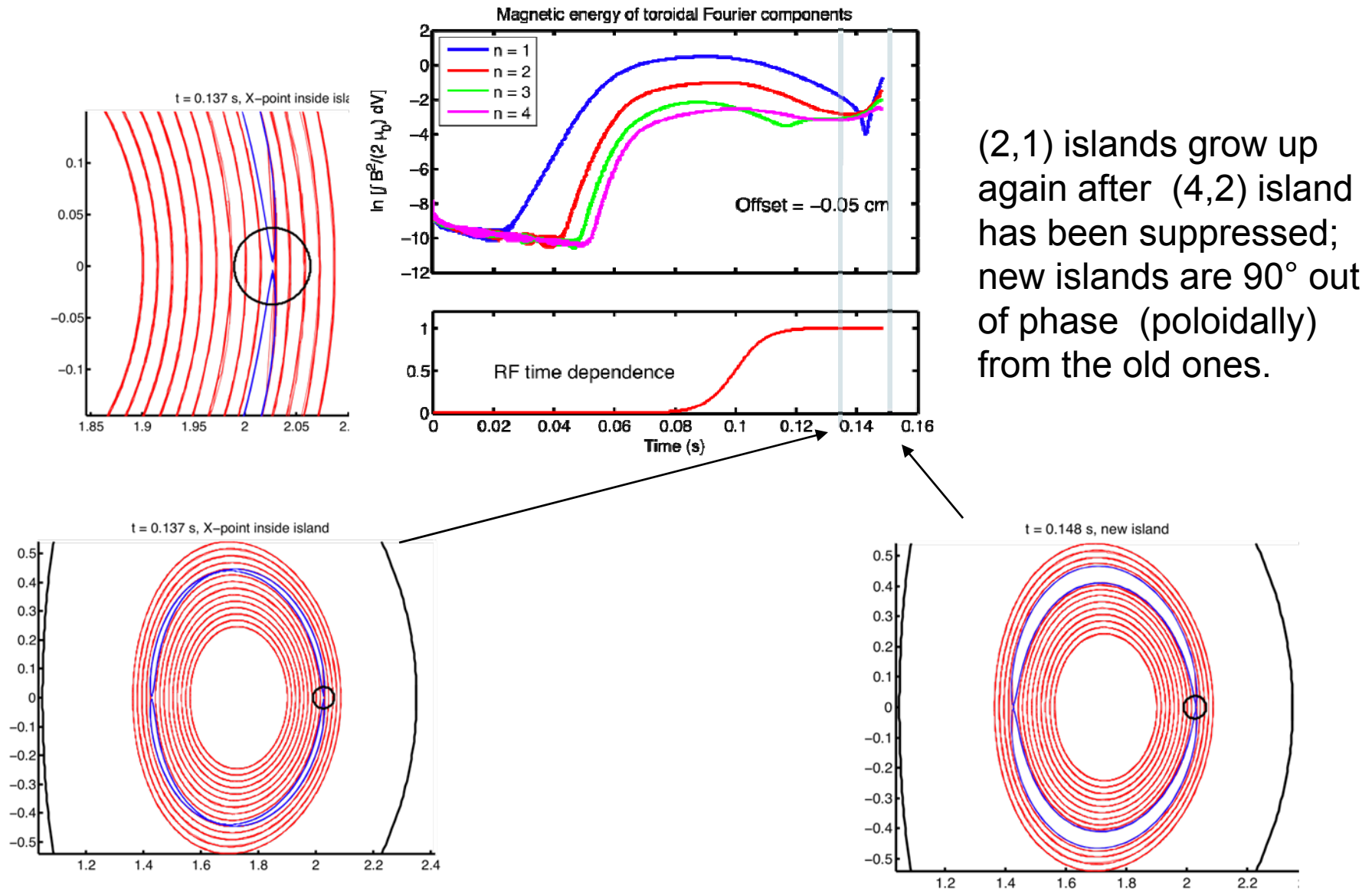
Model current drive source applied to original O-point in 1 toroidal location.

(2,1) island shrinks, becomes (4,2)

(4,2) island shrinks, (2,1) grows

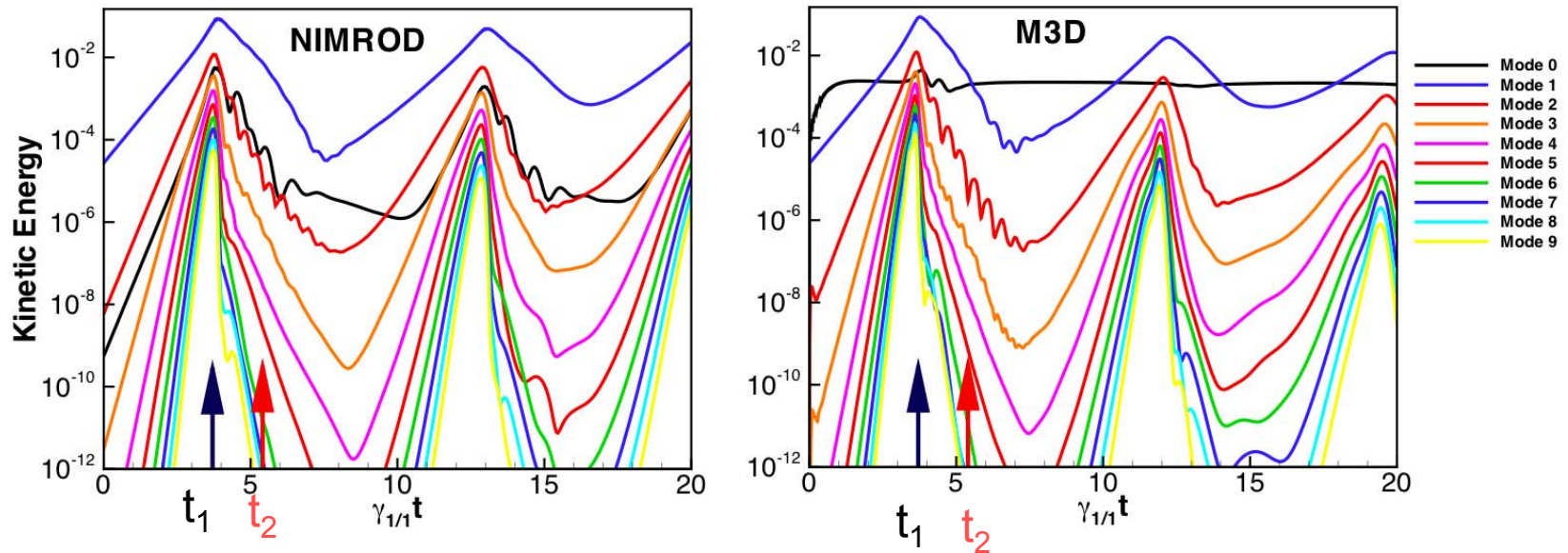
New (2,1) 90° out of phase with old

# As RF suppresses the original islands, new islands arise



(2,1) islands grow up again after (4,2) island has been suppressed; new islands are  $90^\circ$  out of phase (poloidally) from the old ones.

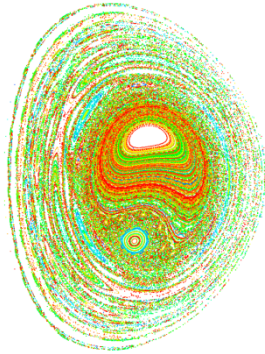
# CDX-U Nonlinear Sawtooth Benchmark demonstrated good agreement between M3D and NIMROD for 3 sawtooth cycles



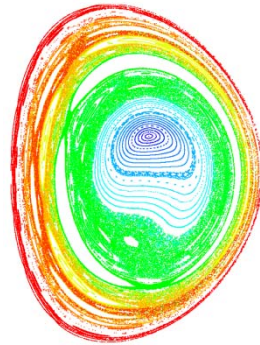
- Figure shows kinetic energy vs time for each of first 10 toroidal modes for nonlinear NIMROD and M3D calculations with same initial conditions, sources, and boundary conditions
- Codes now are in very good agreement in most all aspects (difference in  $n=0$  energy due to different treatment of equilibrium in the 2 codes)
- Times  $t_1$  and  $t_2$  displayed in next vg

# CDX-U Nonlinear Benchmark - 2

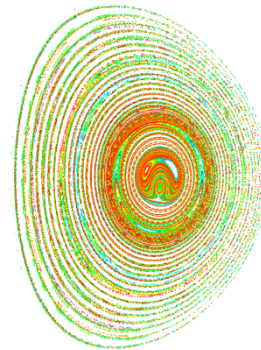
Flux surfaces (Poincaré plots)



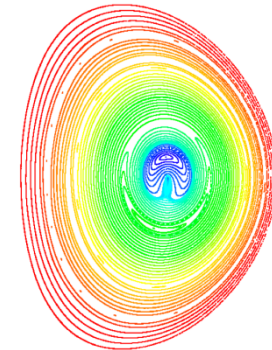
$t=t_1$  (M3D)



$t=t_1$  (NIMROD)

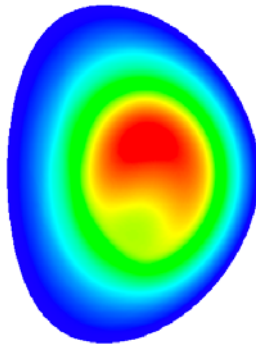


$t=t_2$  (M3D)

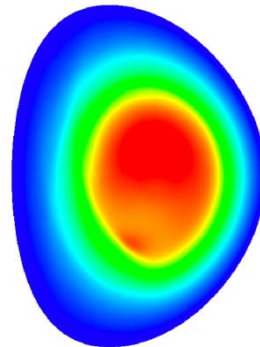


$t=t_2$  (NIMROD)

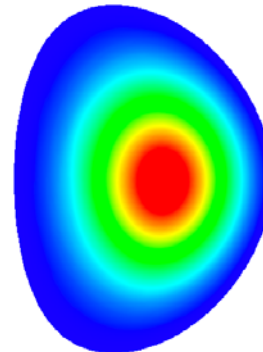
Temperature contours



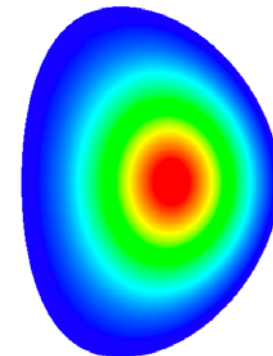
$t=t_1$  (M3D)



$t=t_1$  (NIMROD)

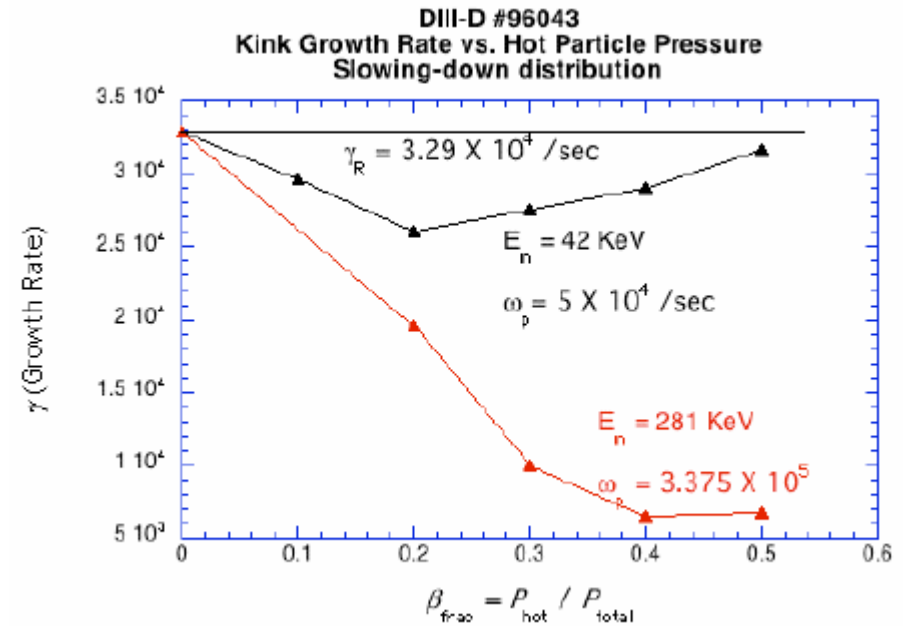
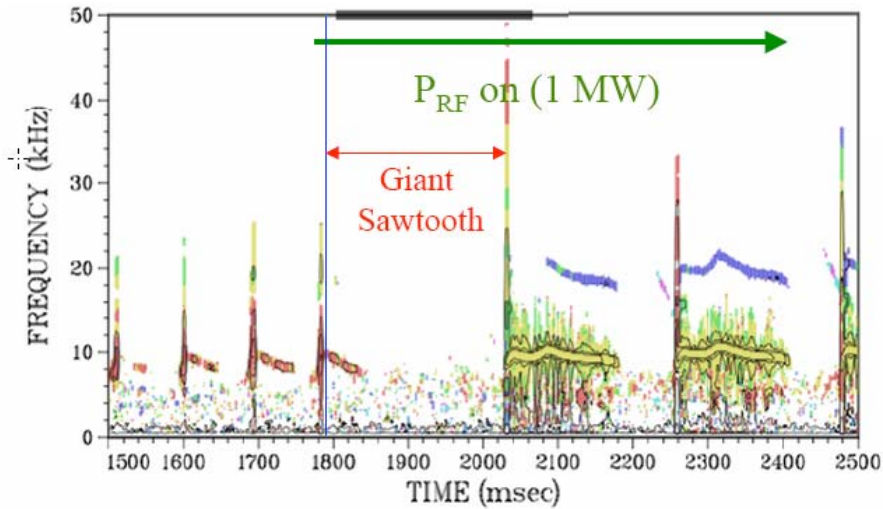


$t=t_2$  (M3D)



$t=t_2$  (NIMROD)

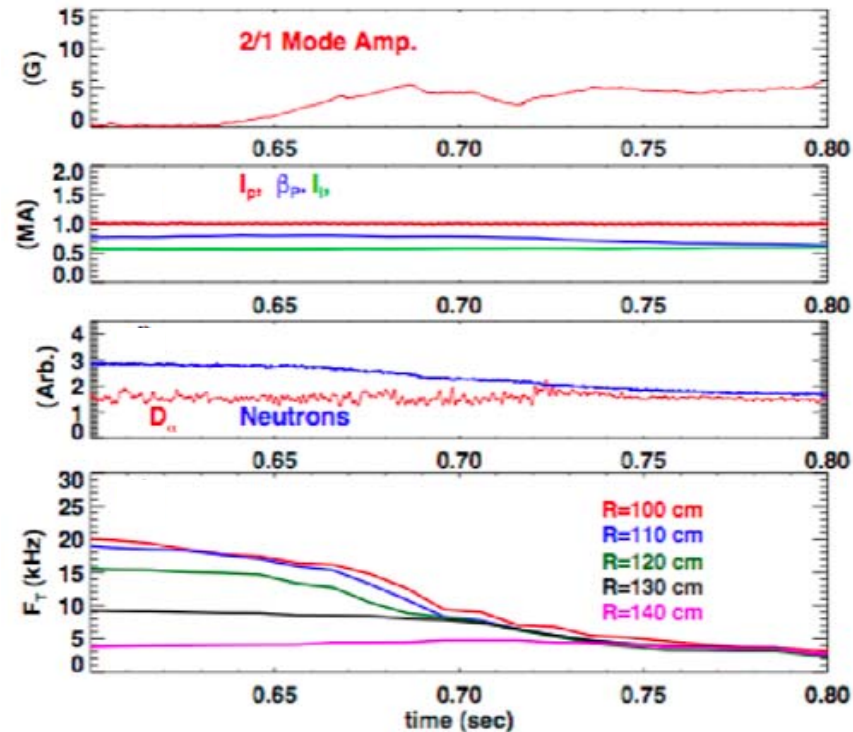
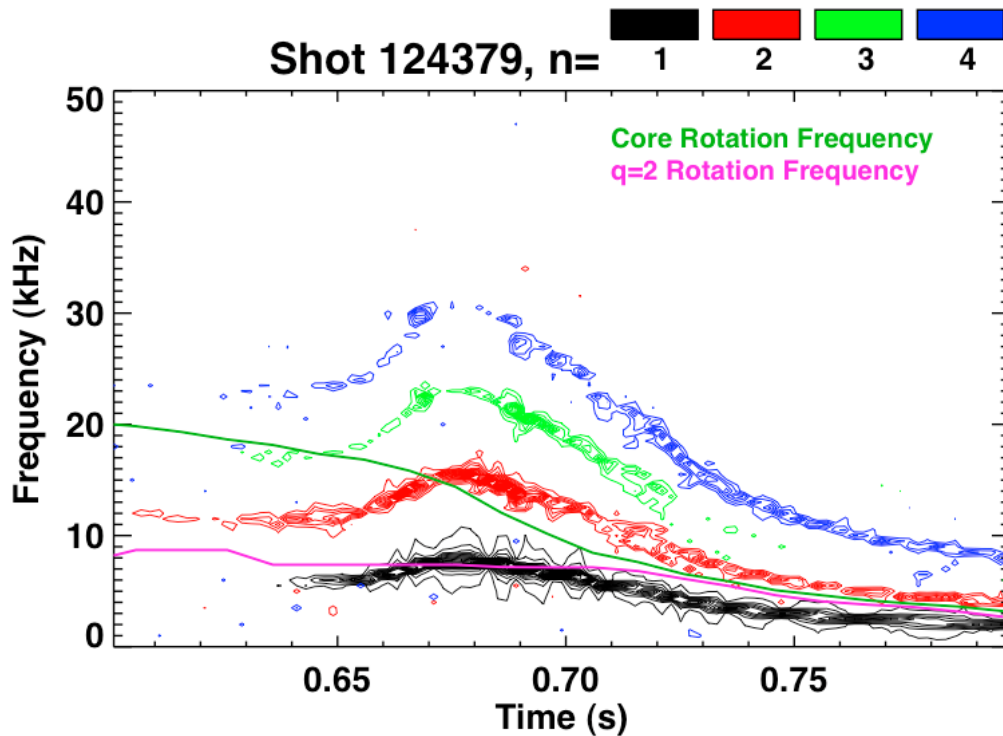
# NIMROD is being used to study Giant Sawtooth in DIII-D



- Hybrid particle/fluid model in NIMROD and M3D
- Shows clear stabilizing effect due to energetic particles, but do not yet have detailed agreement with experiment.

# Study of saturated mode in NSTX-Motivation

NSTX shot 124379 has a steadily growing 2,1 mode with no apparent trigger seen by the USXR,  $D_{\alpha}$ , or neutron diagnostics.

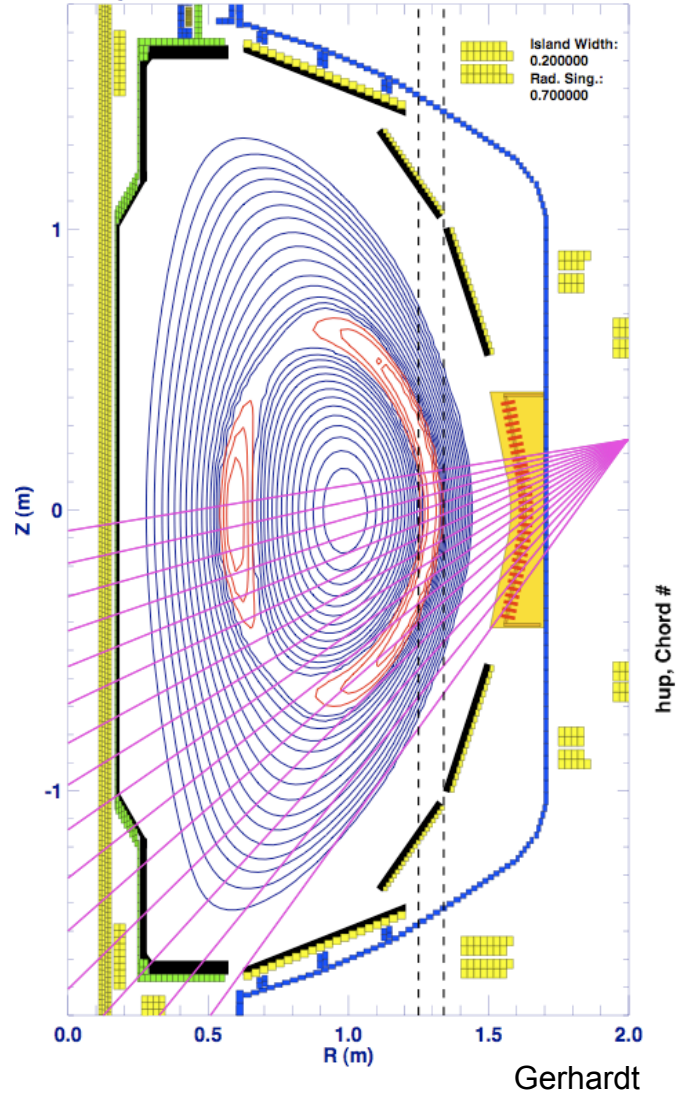


Gerhardt

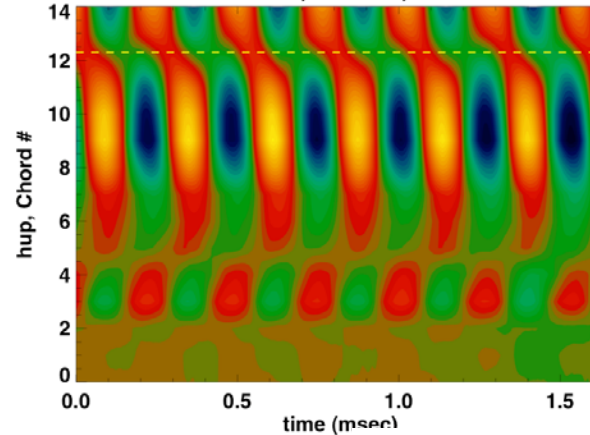


# Eigenfunction Analysis of Multichord Data Suggests Coupling to 1,1 Ideal Kink

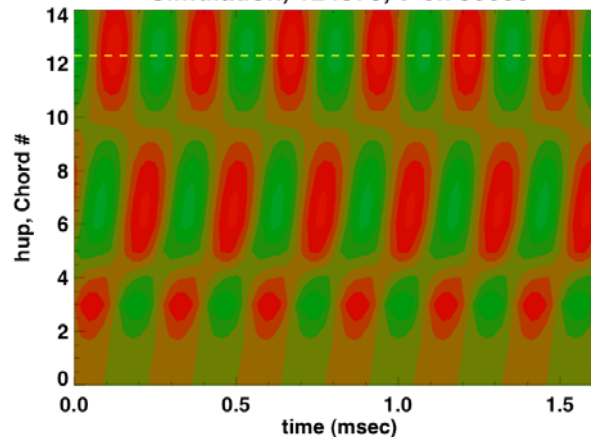
Island Equilibrium and USXR Chords, 124379,  $t=0.730000$



Measurement, 124379,  $t=0.730000$

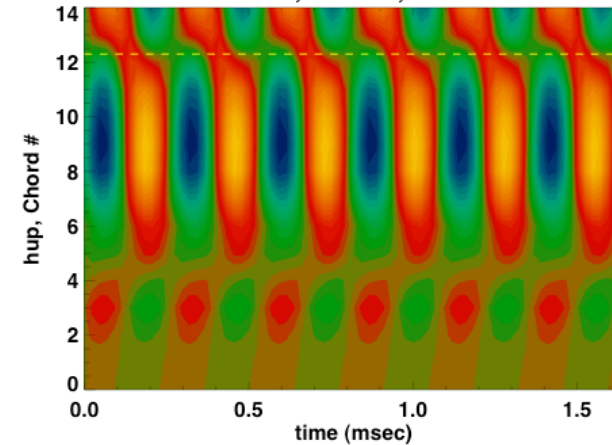


Simulation, 124379,  $t=0.730000$



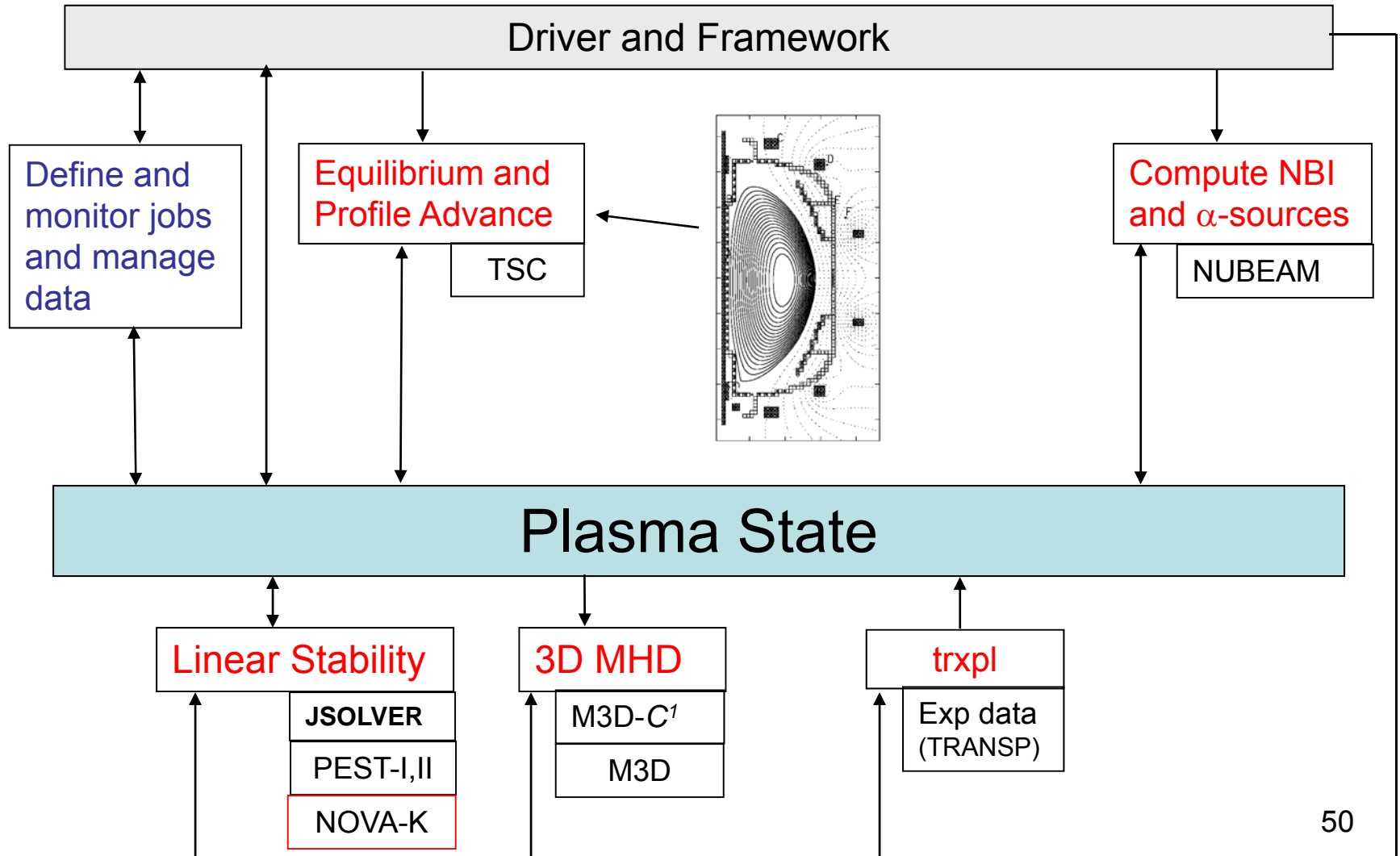
2,1 only

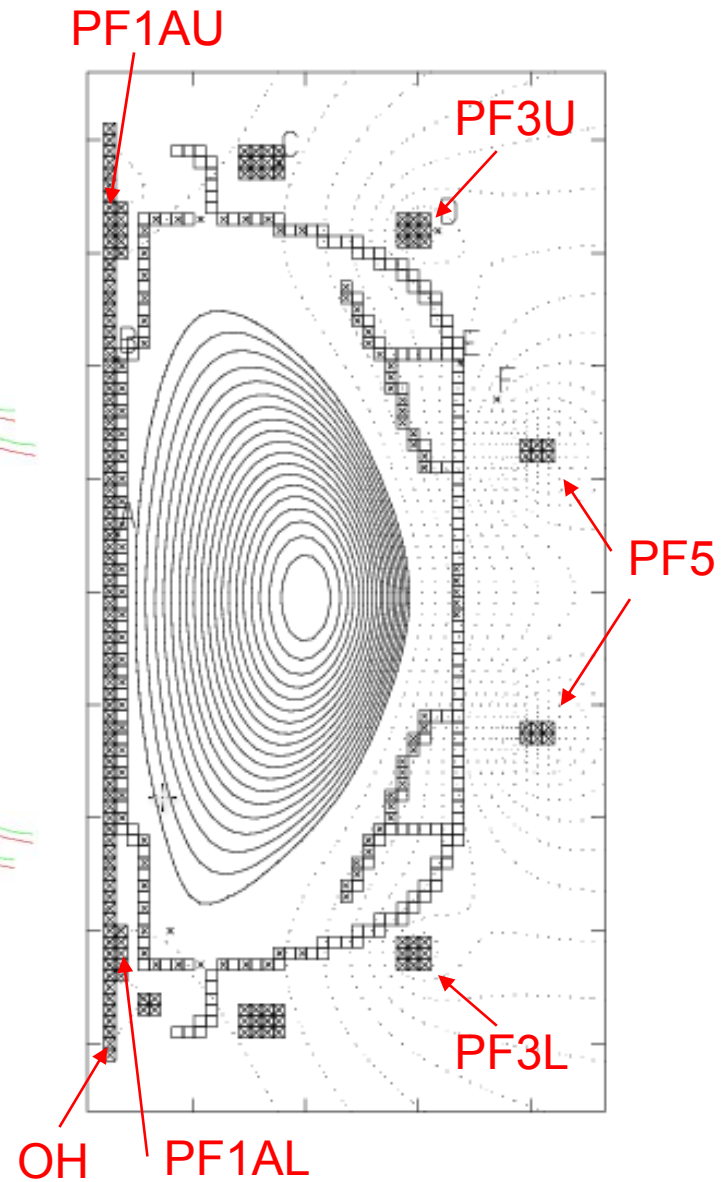
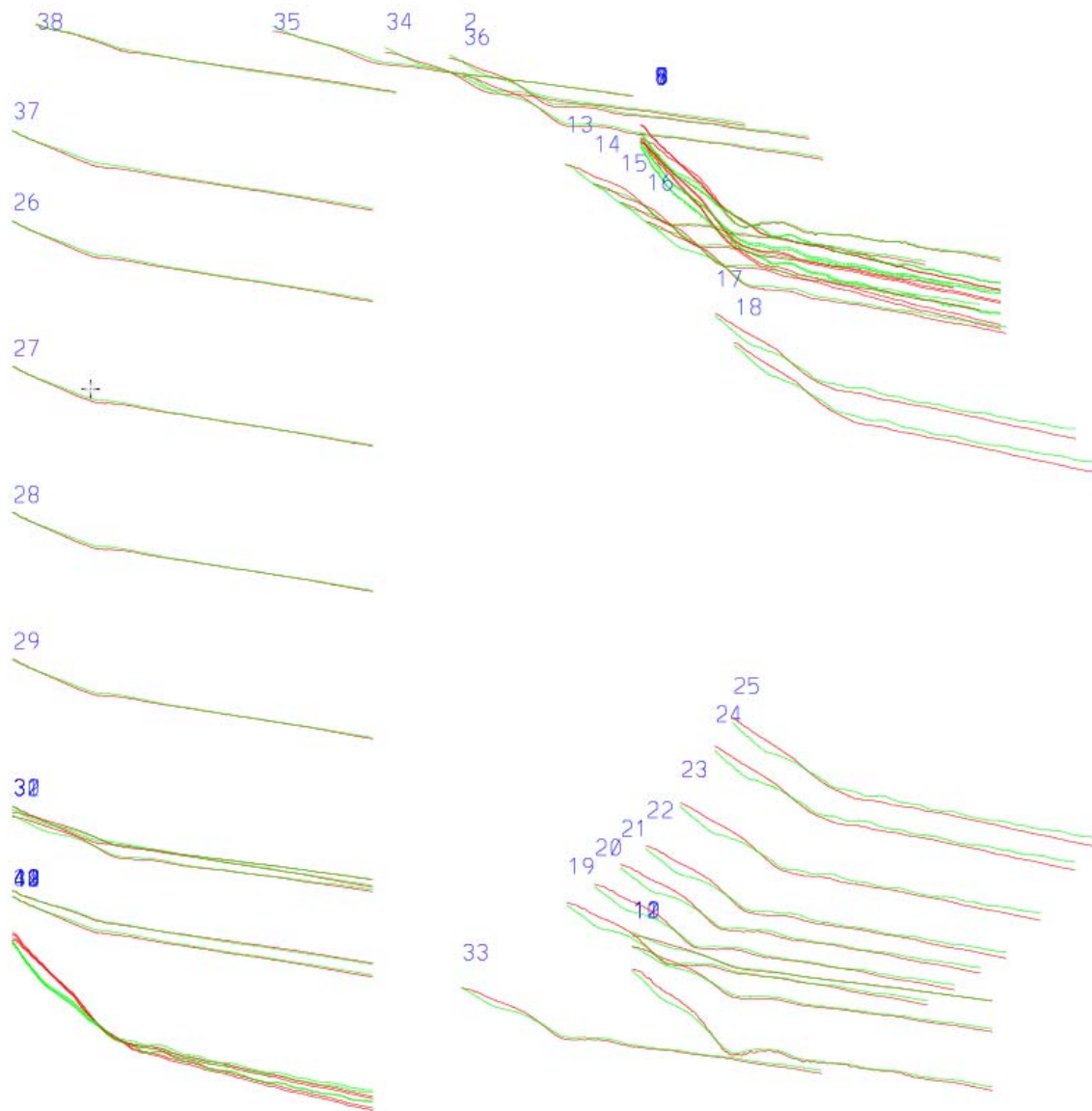
Simulation, 124379,  $t=0.730000$



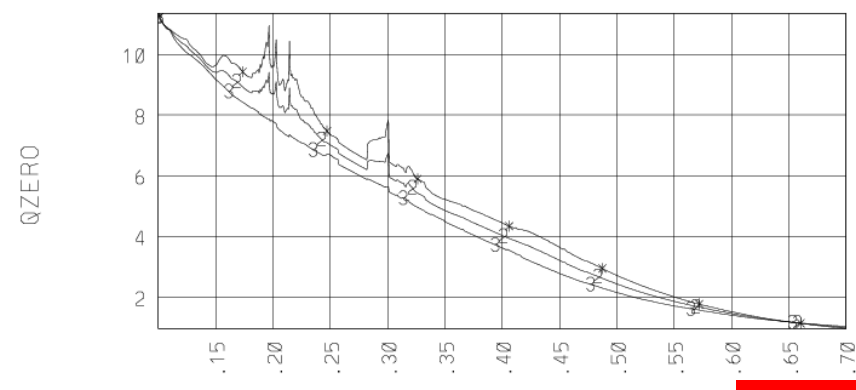
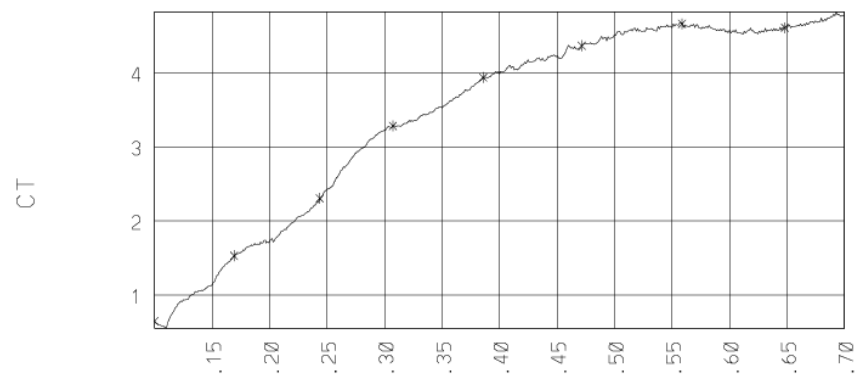
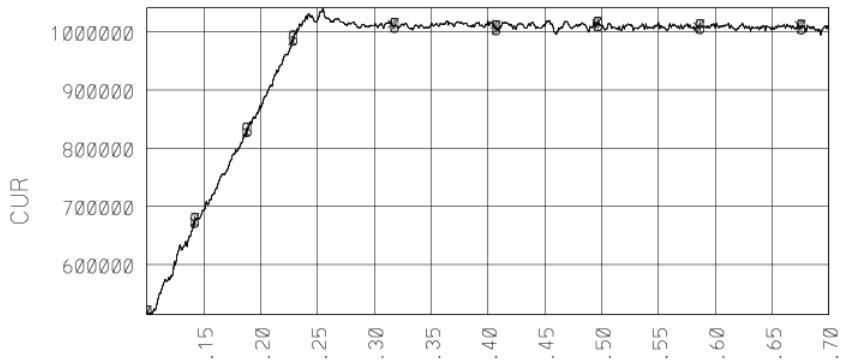
2,1 + 1,1 pert

Now using the SWIM framework to run the free boundary transport code, TSC, using experimental coil currents, and TRANSP Neutral Beam package and monitor stability.

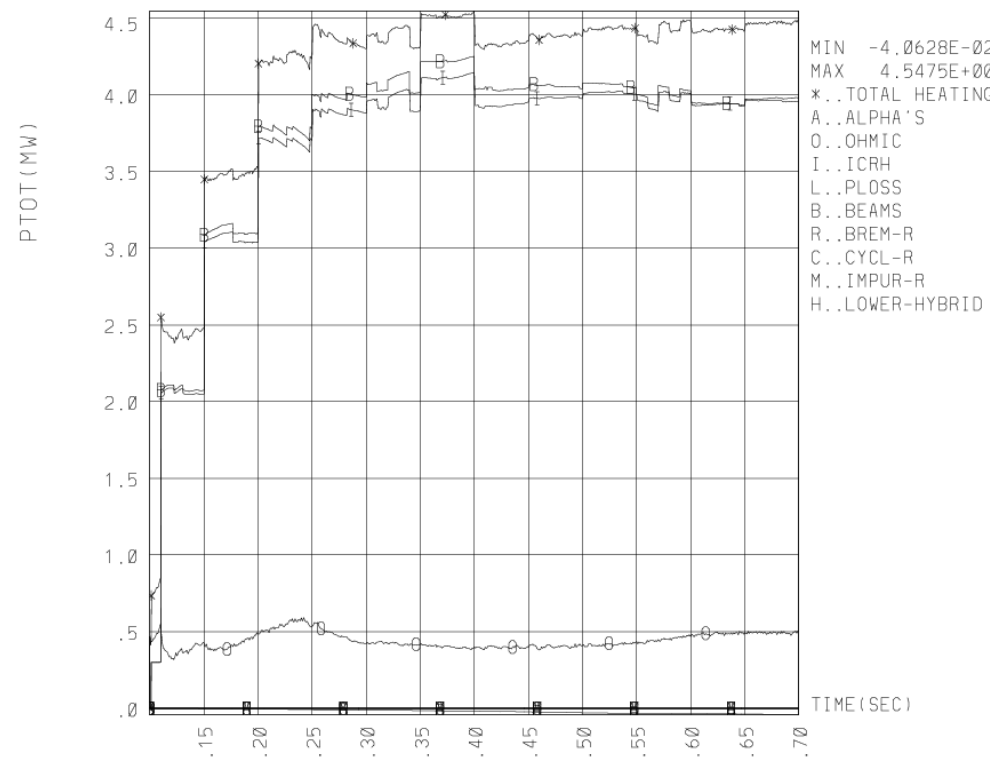




Red are simulation flux loop data and green are experimental data. Origin of each curve is approximate position of flux loop around machine.

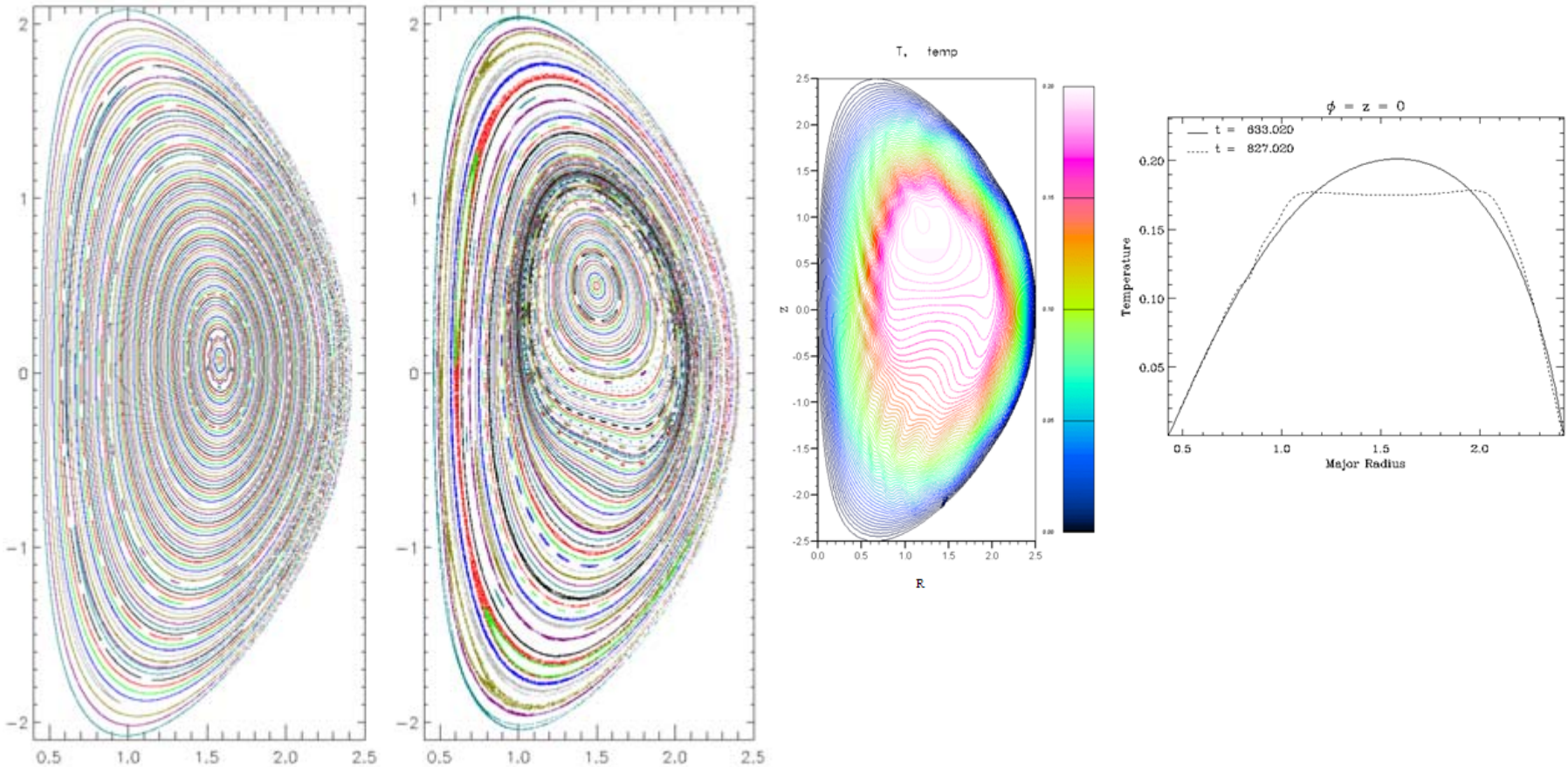


This is the time and the  $q_0$  value when the instability sets in



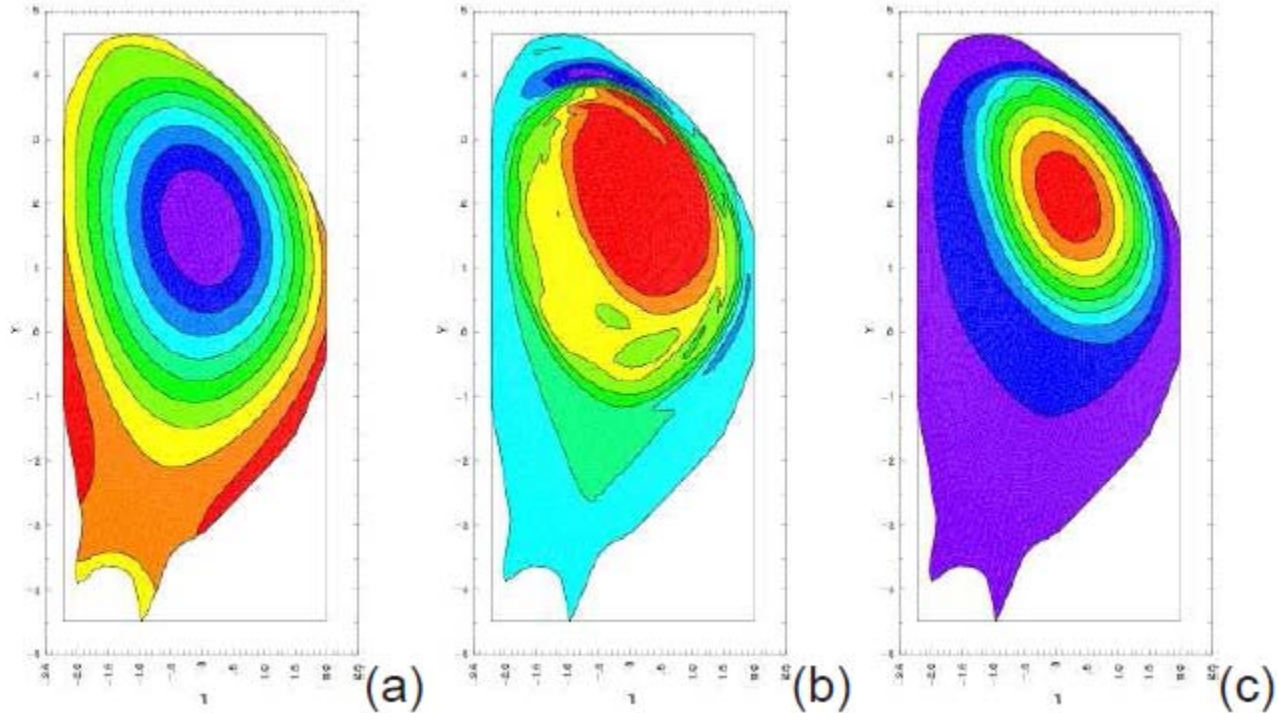
4MW of beams is applied from the beginning, but the low initial density leads to initial shine-through

# M3D simulation of saturated mode in NSTX when $q_0 > 1$



Saturated  $n=1$  mode can set develop when  $q_0$  slightly  $> 1$ , as seen in Poincare plot on left. Can flatten temperature (right) and also drive  $m=2$  islands.  
Breslau, et al. IAEA 2010

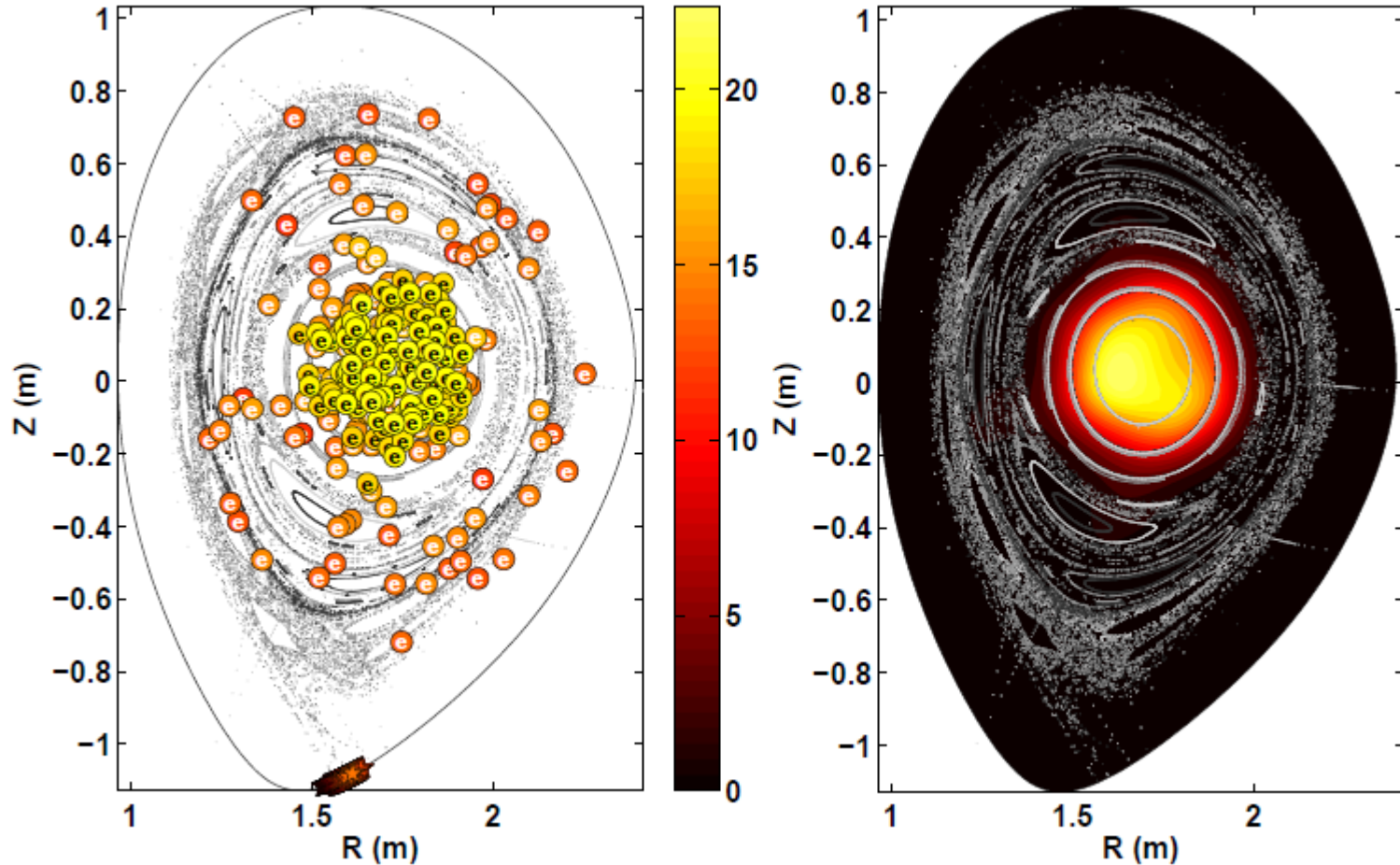
# VDE<sup>1</sup> and Plasma Disruption simulations in ITER



(a) Poloidal flux, (b) toroidal current, and (c) temperature during a vertical displacement event. A VDE brings the plasma to the upper wall where a  $(m,n) = (1,1)$  kink mode grows. Forces on the vacuum vessel are calculated.

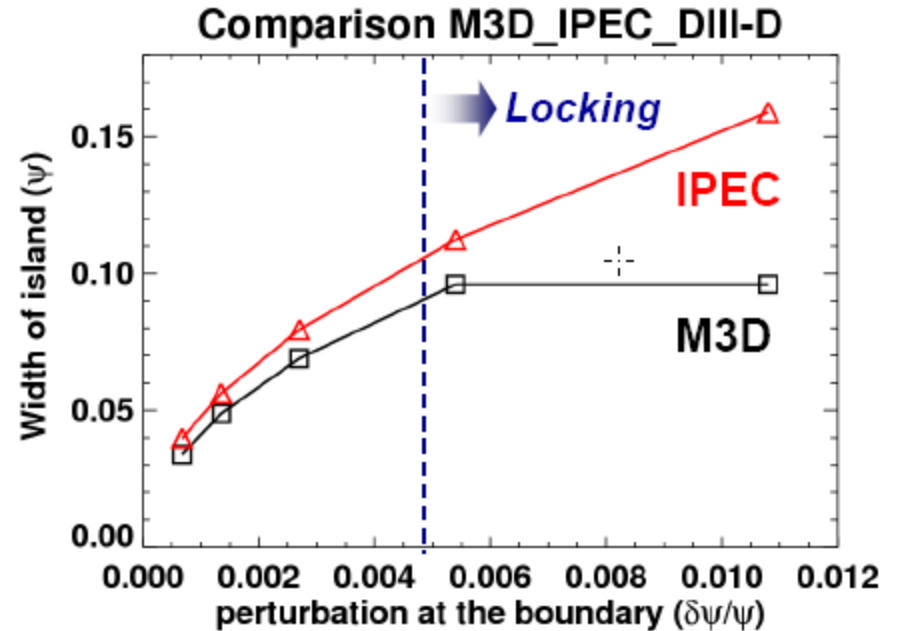
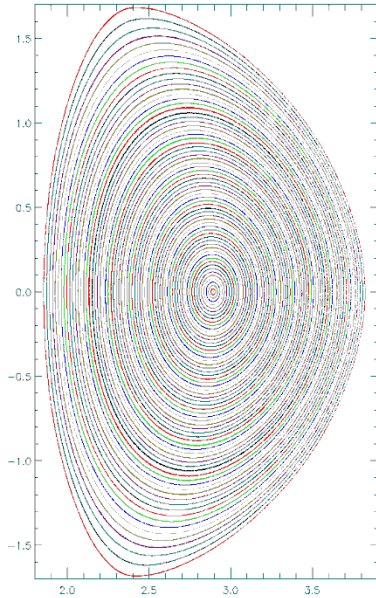
<sup>1</sup>Vertical Displacement Event

Runaway electron evolution in disrupting plasma is computed.



Simulation of DIII-D Ar pellet experiments. Runaway electrons of different energy shown. Synchrotron emission on right.

# Error Field study



$$q_{\min} = 1.067$$

$$q_{\text{edge}} \sim 4$$

$$\tilde{\psi}_{\text{boundary}}(\theta, \varphi) = \tilde{\psi}_0 \cos(\varphi - 2\theta)$$

Non-linear non-ideal M3D code has been used to extend the IPEC results:

- Islands growth due to error fields in the presence of rotation is found to be very complex. Requires accurate model of viscous damping, etc. Still under investigation.



# Summary

- 2D studies
- Edge localized modes (ELMs)
  - Linear benchmarking
  - Nonlinear evolution (with CPES)
- Tearing modes
  - Linear studies at high S
  - Nonlinear evolution and stabilization (with SWIM)
- Sawtooth and other (1,1) modes
  - Nonlinear benchmarking study with CDX-U
  - Approach to mode onset in NSTX (with SWIM)
  - Giant sawtooth in DIII-D
- Disruptions and resistive wall mode (RWM)
- Error field studies



Jardin

Chapman & Hall/CRC  
Computational Science Series

# Computational Methods in Plasma Physics

Stephen Jardin

Computational Methods in Plasma Physics

 **CRC Press**  
Taylor & Francis Group  
an informa business  
[www.crcpress.com](http://www.crcpress.com)

CRC Press, Taylor & Francis Group  
270 Madison Avenue  
New York, NY 10017  
2 Park Square, Milton Park  
Abingdon, Oxon OX14 4RN, UK



 **CRC Press**  
Taylor & Francis Group  
A CHAPMAN & HALL BOOK